

CP Asymmetries in $B \rightarrow f_0 K_S$ Decays

Rupak Dutta^{1*} and Susan Gardner^{2†}

^{1,2}*Department of Physics and Astronomy,
University of Kentucky,
Lexington, Kentucky 40506-0055*

Abstract

We consider the branching ratio and the CP asymmetries in $B \rightarrow f_0(980)K_S$ decay to the end of determining the deviation of the time-dependent CP asymmetry from $\sin(2\beta)$, $\Delta S_{f_0 K_S} \equiv -\eta_{f_0 K_S} S_{f_0 K_S} - \sin(2\beta)$, arising from Standard Model physics. We obtain $\Delta S_{f_0 K_S}$ within the context of the QCD factorization framework for the $B \rightarrow f_0(980)K_S$ decay amplitudes assuming the $f_0(980)$ is a $q\bar{q}$ state and employing a random scan over the theoretical parameter space to assess the possible range in $\Delta S_{f_0 K_S}$. Imposing the value of the experimental branching ratio within 1σ and 3σ , respectively, of its central value as a constraint, we find the range of $\Delta S_{f_0 K_S}$ to be $[0.018, 0.033]$ for a scan in which the parameters are allowed to vary within 1σ of their central values and the range $[-0.019, 0.064]$ for a scan in which the parameters vary within 3σ of their central values.

*Electronic address: rdutta@uky.edu

†Electronic address: gardner@pa.uky.edu

I. INTRODUCTION

In the Standard Model (SM), all CP-violating effects derive from a single, complex phase of the Cabibbo-Kobayashi-Maskawa (CKM) matrix and predicate a distinctive pattern of CP-violation [1]. For example, in the decay of a B-meson to a CP-eigenstate f , the time-dependent asymmetry S_f realized from $b \rightarrow sc\bar{c}$ decay determines $\sin(2\beta)$, where β is given by $\beta = \arg(-V_{cd}V_{cb}^*/V_{td}V_{tb}^*)$ and V_{ij} is a CKM matrix element [2, 3, 4]. This quark-level transition can be studied in a variety of B-meson decays, and departures of the determined time-dependent asymmetry from $\sin(2\beta)$ could signal the presence of non-SM physics, which may occur in $B - \bar{B}$ mixing, in the decay amplitude, or in both [5].

In this paper, we consider the decay $B \rightarrow f_0(980)K_S$, which is mediated by the $b \rightarrow sq\bar{q}$ transition at one-loop-order in the weak interaction. The decay $B \rightarrow f_0(980)K_S$ is one of several penguin-dominated modes which probe $\sin(2\beta)$. In contrast, in $B \rightarrow J/\psi K_S$ decay, and related charmonium modes, the $b \rightarrow sc\bar{c}$ transition operates at tree level. Were the time-dependent asymmetries in tree- and penguin-dominated modes to differ, then non-SM physics could be at work in the penguin process [6]. Current experimental results suggest that this could be the case [7], though definite conclusions require both experimental results of improved precision and theoretical estimates of the subleading SM corrections. The numerical size of the SM corrections depend on the specific decay mode, mimicking the appearance of non-SM physics [8], so that the needed estimates demand some care. In this context it is worth noting that the “wrong phase” penguin contribution, proportional to the weak phase of $b \rightarrow su\bar{u}$, is particularly small in $B \rightarrow J/\psi K_S$ decay; indeed, the deviation of the time-dependent asymmetry $S_{J/\psi K_S}$ from $\sin(2\beta)$ is $\mathcal{O}(10^{-3})$ [9, 10] — it is suppressed by both CKM and loop effects. Thus the comparison of this asymmetry to a “tree-only” determination of $\sin(2\beta)$ permits a sensitive assay of new physics in $B^0 - \bar{B}^0$ mixing. Currently this last is consistent with $S_{J/\psi K_S}$, as well as with other determinations of $\sin(2\beta)$ which employ information on the sides of the unitarity triangle, at the $\mathcal{O}(10\%)$ level [11, 12]. In the case of the penguin modes, the wrong-phase penguin is larger as it is suffers only CKM, i.e., $\mathcal{O}(\lambda^2) \simeq 0.04$, suppression. In these modes the computed SM deviations from $\sin(2\beta)$ determine a much-needed baseline against which the experimental results can be assessed for new-physics effects, as new-physics-induced deviations from $\sin 2\beta$ could certainly be channel-dependent as well. Systematic studies of the SM corrections exist [13, 14, 15] in a variety of modes. The $B \rightarrow f_0(980)K_S$ mode has received less attention, perhaps due to the ill-known quark structure of the $f_0(980)$ [16, 17]; this is a deficiency we wish to remedy.

The $f_0(980)$ is a fairly narrow resonance of non-Breit-Wigner form which couples to $\pi\pi$ and $K\bar{K}$ final states. The quark structure of the $f_0(980)$ meson is not well established. Much discussion has revolved around whether it is better regarded as a $q^2\bar{q}^2$ state [18] or, perhaps, as a $K\bar{K}$ molecule [19, 20]. The theoretical correction relevant to the interpretation of $S_{f_0 K_S}$ as a measurement of $\sin 2\beta$ comes from the presence of the $b \rightarrow su\bar{u}$ transition in the decay amplitude, and interconnected issues complicate its analysis. Not only must we consider the possible non- $q\bar{q}$ structure of the f_0 resonance, but we must also recall that strong final-state interactions exist in $\pi\pi$ scattering in the $I = 0, J = 0$ channel [21, 22, 23]. Such final-state interactions give rise to the scalar form factor, and particularly the partial width $\Gamma(f_0(980) \rightarrow \pi\pi, K\bar{K})$, which can be computed through

the unitarization of a scattering kernel compatible with low-energy constraints [24, 25, 26]. We presume the $f_0(980)$ resonance to be sufficiently narrow relative to the energy released in the B decay that we can approximate the full decay amplitude as the product of the two-body decay amplitude $A(B \rightarrow f_0(980)K_S)$ with $\Gamma(f_0(980) \rightarrow \pi\pi, K\bar{K})$, where we refer to Ref. [27] for a discussion of the assumptions implicit to this treatment. In particular, the strong phases associated with the long-distance physics of f_0 decay are presumed to be universal and not modified by the B-decay environment, so that the decay-specific phases are captured by the application of QCD perturbation theory in the heavy quark limit to the two-body decay process. Corrections to the picture we employ can be estimated, though not in a systematically improvable way. For example, so-called final-state rescattering has been estimated for various $b \rightarrow s$ penguin modes [15], and OZI-violating effects can also be considered, the latter contributing significantly to $J/\psi \rightarrow \phi\pi\pi$ decay, e.g. [25, 26]. We reserve discussion of the impact of the computed $f_0 \rightarrow \pi\pi$ and $f_0 \rightarrow K\bar{K}$ partial widths, as well as of possible OZI-violating effects, to a subsequent publication [28]. Our particular focus is in the study of the sensitivity of our prediction of the CP asymmetries to the assumed quark structure of the $f_0(980)$; the latter enters in the evaluation of the hadronic matrix elements of the $b \rightarrow su\bar{u}$ transition. A priori one might think such effects to be most important in the assessment of the deviation of $S_{f_0K_s}$ from $\sin(2\beta)$. We proceed in the same vein as Cheng and collaborators [16, 17], treating the $f_0(980)$ as a $q\bar{q}$ state and employing the QCD factorization approach [29, 30] for the hadronic matrix elements. We differ from this earlier work in the treatment of the $B \rightarrow f_0$ form factor. We then perform a random scan over the theoretical parameter space, after Beneke [14], to assess, in part, the sensitivity of the results to the employed hadronic matrix elements and hence to the implicitly assumed structure of the $f_0(980)$.

Let us give a brief outline of this paper. We begin, in Sec. II, with a description of the theoretical framework and briefly review the role of the $b \rightarrow sq\bar{q}$ transition, with $q \in u, d$, in the determination of the CP-violating parameters S_f and C_f , as well as of the two-body branching ratio. We present a synopsis of the pertinent QCD factorization formulae as well. In Sec. III we present the input parameters we use in our numerical calculations, reporting the CP-violating parameters which result from the use of our defined “default” set of input parameters. It should be emphasized that the factorization theorem from which the QCD factorization approach follows holds only at leading power in the heavy quark mass, and the estimate of $1/m_b$ power suppressed terms, though of apparent phenomenological importance, is uncertain. Thus our random scan over the theoretical parameter space, effected to explore the possible range of $\Delta S_{f_0K_S}$ and $C_{f_0K_S}$, takes both uncertainties in the theoretical inputs and in the assessment of the $\mathcal{O}(\Lambda_{QCD}/M_B)$ corrections into account. We report these results in Sec. III as well. We conclude with a summary of our results and an outlook on future work in Sec. IV.

II. THEORETICAL FRAMEWORK

We pattern our analysis after that of Beneke, Ref. [14], and, indeed, adopt a common notation. In particular, we employ the QCD factorization framework [29, 30] for the computation of the $B \rightarrow f_0K_S$ matrix elements [17] and perform a random scan over the space of possible input parameters to estimate the uncertainty in their computation. We begin by recalling that the CP

asymmetry $A_f(t)$ into a CP eigenstate f is given by

$$A_f(t) = \frac{\text{Br}(\bar{B}^0(t) \rightarrow f) - \text{Br}(B^0(t) \rightarrow f)}{\text{Br}(\bar{B}^0(t) \rightarrow f) + \text{Br}(B^0(t) \rightarrow f)} \equiv S_f \sin(\Delta M_B t) - C_f \cos(\Delta M_B t). \quad (1)$$

Here we have neglected $\Delta\Gamma$ where $\Delta\Gamma \equiv \Gamma_H - \Gamma_L$ is the width difference of the B eigenstates. We note $\Delta M_B \equiv M_H - M_L$ is the mass difference of the B eigenstates, S_f is the CP asymmetry generated by the interference of $B - \bar{B}$ mixing and direct decay, and C_f is an asymmetry reflective of direct CP violation. We recall [1]

$$S_f = \frac{2 \text{Im}\lambda_f}{1 + |\lambda_f|^2} \quad ; \quad C_f = \frac{1 - |\lambda_f|^2}{1 + |\lambda_f|^2}, \quad (2)$$

where

$$\lambda_f = \left(\frac{q}{p}\right)_B \frac{A(\bar{B}^0 \rightarrow f)}{A(B^0 \rightarrow f)}, \quad (3)$$

with the factor $(q/p)_B$ characterizing $B - \bar{B}$ mixing. If we treat the $f_0(980)$ resonance as if it were a stable particle, as in Ref. [17], then $f \equiv f_0(980)K_S$, and we write

$$\lambda_{f_0K_S} = \left(\frac{q}{p}\right)_B \left(\frac{q}{p}\right)_K \frac{A(\bar{B}^0 \rightarrow f_0\bar{K}^0)}{A(B^0 \rightarrow f_0K^0)}, \quad (4)$$

where the factor $(q/p)_K$ characterizes $K - \bar{K}$ mixing. In this event, f is a two-body final state, and we write the decay amplitude as

$$A(\bar{B} \rightarrow f) = \lambda_c a_f^c + \lambda_u a_f^u \propto (1 + e^{-i\gamma} d_f), \quad (5)$$

with $d_f \equiv |\lambda_u/\lambda_c|(a_f^u/a_f^c)$ and $\lambda_q \equiv V_{qb}V_{qs}^*$ for $q \in u, c$ to determine

$$\Delta S_f \equiv -\eta_f S_f - \sin(2\beta) = \frac{2 \text{Re}(d_f) \cos(2\beta) \sin \gamma + |d_f|^2 (\sin(2\beta + 2\gamma) - \sin(2\beta))}{1 + 2 \text{Re}(d_f) \cos \gamma + |d_f|^2}, \quad (6)$$

where η_f is the eigenvalue of the CP-operator associated with the eigenstate f . Moreover, we have

$$C_f = -\frac{2 \text{Im}(d_f) \sin \gamma}{1 + 2 \text{Re}(d_f) \cos \gamma + |d_f|^2}, \quad (7)$$

so that if $|d_f|$ is small, the functions ΔS_f and C_f show little correlation [14]. The value of ΔS_f in the SM shows certain systematic trends with f [14]. For example, if a color-suppressed tree amplitude C contributes to a_f^u , then ΔS_f is much larger than it would be if it were absent. In the latter event, the u -quark penguin amplitude P^u drives a_f^u . Generally, $d_f \propto (\pm C + P^u)/P^c$. If the parameters describing the $B \rightarrow f$ decay amplitude make $|P^c|$ small relative to $|C|$, then ΔS_f can range over a wide array of values. Such large excursions can be controlled, however, by demanding that the amplitudes be consistent with the empirical branching ratios [14]. In the case of current interest, $B \rightarrow f_0K_S$ decay, there is no C amplitude, so that we expect $\Delta S_{f_0K_S}$ to be small on general grounds, and the imposition of a branching ratio constraint should no longer be crucial. However, we have found exceptional regions in theoretical parameter space for which P^c is small with respect

to P^u and thus $\Delta S_{f_0 K_S}$ is large, so that it is, in fact, crucial to apply the branching ratio constraint to eliminate these large excursions.

If we treat $\bar{B}^0 \rightarrow f_0(980)\bar{K}^0$ decay as a two-body process, then the decay rate is

$$\Gamma = \frac{p}{8\pi M_B^2} |\mathcal{M}|^2, \quad (8)$$

where $\mathcal{M} \equiv A(\bar{B}^0 \rightarrow f_0\bar{K}^0)$, as we shall describe in detail, and

$$p = \frac{\sqrt{(M_B^2 - (M_{f_0} + M_{K^0})^2)(M_B^2 - (M_{f_0} - M_{K^0})^2)}}{2M_B}. \quad (9)$$

We recall that the branching ratio is given by Γ/Γ_B , where Γ_B is the total decay width of B meson. In reality, the $f_0(980)$ is not a stable particle; rather, it is a resonance which decays to both $\pi\pi$ and $K\bar{K}$ final states. We wish to investigate the role of finite-width effects explicitly in a subsequent publication [28]: we neglect them here. To begin, we rewrite the two-body decay amplitude as

$$A(\bar{B} \rightarrow f_0\bar{K}_0) = A_u^n \lambda_u + A_c^n \lambda_c + A_u^s \lambda_u + A_c^s \lambda_c, \quad (10)$$

where the superscript (n, s) refers to the non-strange and strange quark components of the $f_0(980)$, respectively, so that

$$d_{f_0 K_S} = \left| \frac{\lambda_u}{\lambda_c} \right| \left(\frac{A_u^n + A_u^s}{A_c^n + A_c^s} \right). \quad (11)$$

We now proceed to calculate the $A_{u,c}^{n,s}$ amplitudes.

A. $\bar{B} \rightarrow f_0\bar{K}$ Decay in QCD Factorization

The decay amplitudes of exclusive hadronic B -meson decays can be systematically analyzed in a combined expansion of inverse powers of the heavy quark mass m_b and the strong coupling constant α_s [31, 32, 33]. The QCD factorization approach, in specific, permits the rigorous computation of these amplitudes, for certain two-body final states, in leading power in $\mathcal{O}(\Lambda_{QCD}/m_b)$ and in a power series in $\alpha_s(\mu)$, where $\mu \sim \mathcal{O}(m_b)$ [29]. Its starting point is the effective weak Hamiltonian for charmless hadronic B decay, consisting of a sum of the products of CKM matrix elements, local operators Q_i , and Wilson coefficients $C_i(\mu)$, evaluated in next-to-leading order (NLO) precision in $\alpha_s(\mu)$ [34]. Some dissension in the literature exists concerning the ingredients of the leading power analysis [35], particularly in regards to the charm-quark penguin contributions [36, 37]: in the QCD factorization approach any non-factorizable charm-quark penguin contributions appear in $\mathcal{O}(\Lambda_{QCD}/m_b)$ corrections. Although recent work suggests that such charm-quark penguin effects may be needed to explain the B -decay data to light charmless mesons [38], note also Ref. [39], in our context we can safely neglect such developments, as they cannot make $\Delta S_{f_0 K_S}$ larger. B -meson decays to scalar- and pseudoscalar-meson final states have recently been studied by Cheng and collaborators in a series of papers [15, 16, 17]; they employ the QCD factorization approach and treat the $f_0(980)$ resonance as a $q\bar{q}$ state. Their results connect to those of Beneke and Neubert for B -meson decays to pseudoscalar- and vector-meson final states [30], as the amplitudes for the scalar-

and pseudoscalar-meson channels follow from these earlier results upon a series of replacements [17]. This means that the twist-3 light-front distribution amplitudes are assumed to be determined by two-particle configurations only. The amplitude for $\bar{B}^0 \rightarrow f_0 \bar{K}^0$ decay is given in Ref. [17], so that we identify, after Eq. (10),

$$A_u^n = -\frac{G_F}{\sqrt{2}} \left[\left(a_4^u - r_\chi^K a_6^u - \frac{1}{2}(a_{10}^u - r_\chi^K a_8^u) \right)_{f_0 K} \right] f_K F_0^{B f_0}(M_{K^0}^2)(M_B^2 - M_{f_0}^2) \\ + \frac{G_F}{\sqrt{2}} \left[\left(b_3 - \frac{1}{2} b_{3EW} \right)_{f_0^d K} \right] f_B, \quad (12)$$

$$A_c^n = -\frac{G_F}{\sqrt{2}} \left[\left(a_4^c - r_\chi^K a_6^c - \frac{1}{2}(a_{10}^c - r_\chi^K a_8^c) \right)_{f_0 K} \right] f_K F_0^{B f_0}(M_{K^0}^2)(M_B^2 - M_{f_0}^2) \\ + \frac{G_F}{\sqrt{2}} \left[\left(b_3 - \frac{1}{2} b_{3EW} \right)_{f_0^d K} \right] f_B, \quad (13)$$

$$A_u^s = -\frac{G_F}{\sqrt{2}} \left[\left(a_6^u - \frac{1}{2} a_8^u \right)_{K f_0} \right] \bar{r}_\chi^{f_0} \bar{f}_{f_0}^s F_0^{BK}(M_{f_0}^2)(M_B^2 - M_{K^0}^2) \\ + \frac{G_F}{\sqrt{2}} \left[\left(b_3 - \frac{1}{2} b_{3EW} \right)_{K f_0^s} \right] f_B, \quad (14)$$

$$A_c^s = -\frac{G_F}{\sqrt{2}} \left[\left(a_6^c - \frac{1}{2} a_8^c \right)_{K f_0} \right] \bar{r}_\chi^{f_0} \bar{f}_{f_0}^s F_0^{BK}(M_{f_0}^2)(M_B^2 - M_{K^0}^2) \\ + \frac{G_F}{\sqrt{2}} \left[\left(b_3 - \frac{1}{2} b_{3EW} \right)_{K f_0} \right] f_B. \quad (15)$$

The $M_1 M_2$ subscripts mean that the quantities in brackets are to be interpreted as $a_i^p(M_1 M_2)$, in which the M_1 meson contains the spectator quark from the B -meson, and $b_i(M_1 M_2)$, in which the M_1 meson carries an anti-quark from the weak vertex and the M_2 meson contains a quark from the weak vertex. The QCD factorization framework is rigorous in leading order in $\mathcal{O}(\Lambda_{QCD}/m_b)$, but it also includes estimates of $1/m_b$ -suppressed corrections. We note that $\bar{r}_\chi^{f_0} = 2M_{f_0}/m_b(\mu)$ and $r_\chi^K = 2M_{K^0}^2/(m_b(\mu)(m_s(\mu) + m_d(\mu)))$ but that these chirally-enhanced terms are counted as terms of leading power in the $1/m_b$ expansion in QCD factorization. The quark masses are running masses defined in the \overline{MS} scheme. Certain $1/m_b$ corrections can suffer endpoint divergences, and their estimate is uncertain. The $b_i(M_1 M_2)$ terms, for example, reflect annihilation contributions, which are a class of $1/m_b$ -suppressed corrections to the decay rate. Moreover, the $a_i^p(M_1 M_2)$ terms contain $\mathcal{O}(\alpha_s)$ corrections to the operator matrix elements, which can, in turn, contain $1/m_b$ -suppressed corrections. The $\mathcal{O}(\alpha_s)$ corrections encode non-perturbative input through integrals over the light-cone distribution amplitudes. The coefficients $a_i^p(M_1 M_2)$, where $p = u, c$, can be expressed as [29, 30]

$$a_i^p(M_1 M_2) = C_i(\mu) + \frac{C_{i\pm 1}(\mu)}{N_c} + \frac{C_{i\pm 1}(\mu)}{N_c} \frac{C_{F\alpha_s}(\mu)}{4\pi} \left[V_i(M_2) + \frac{4\pi^2}{N_c} H_i(M_1 M_2) \right] + P_i^p(M_2), \quad (16)$$

where the upper signs apply when i is odd, the lower signs apply when i is even, and $C_F = (N_c^2 - 1)/2N_c$ with $N_c = 3$. The quantities $V_i(M_2)$, $H_i(M_1 M_2)$, and $P_i(M_2)$ reflect vertex corrections, hard spectator interactions, and penguin corrections, respectively. The function $H_i(M_1 M_2)$ contains an endpoint divergence in its power suppressed terms — we refer to Refs. [29, 30] for all omitted details. For work towards a theory of the power corrections, we refer the reader to the developments in Refs. [31, 32, 33]. The coefficients b_i relevant to our calculation can be expressed as [29, 30]

$$\begin{aligned} b_3(M_1 M_2) &= \frac{C_F}{N_c^2} \left[C_3 A_1^i + C_5 (A_3^i + A_3^f) + N_c C_6 A_3^f \right], \\ b_{3,EW}(M_1 M_2) &= \frac{C_F}{N_c^2} \left[C_9 A_1^i + C_7 (A_3^i + A_3^f) + N_c C_8 A_3^i \right], \end{aligned} \quad (17)$$

where in the annihilation amplitudes $A_n^{i,f} \equiv A_n^{i,f}(M_1 M_2)$ the superscripts i and f refer to gluon emission from initial- and final-state quarks, respectively. For the calculation of $A_n^{i,f}(M_1 M_2)$ we include the corrections coming from α_2^K , the second Gegenbauer moment of the kaon, for consistency with our analysis of the $f_0(980)$, and we provide explicit expressions in App. A.

The expressions for $\bar{B} \rightarrow f_0 \bar{K}$ decay contain non-perturbative hadronic input through the meson decay constants and $B \rightarrow M$ form factors; these quantities are sensitive to the assumed quark structure of the hadrons. Assuming the $f_0(980)$ resonance can be written as a $q\bar{q}$ state, we write

$$|f_0(980)\rangle = \cos \theta |s\bar{s}\rangle + \sin \theta |n\bar{n}\rangle, \quad (18)$$

where $|n\bar{n}\rangle \equiv (|u\bar{u}\rangle + |d\bar{d}\rangle)/\sqrt{2}$. The empirical observation of both $\Gamma(J/\psi \rightarrow f_0 \omega)$ and $\Gamma(J/\psi \rightarrow f_0 \phi)$ suggests that the $f_0(980)$ has both strange and non-strange components, so that θ is non-zero [16]. We define the $B \rightarrow f_0$ form factor as

$$\langle f_0(p') | \bar{d} \gamma_\mu \gamma_5 b | B(p) \rangle = -i \left[\left(P_\mu - \frac{M_B^2 - M_{f_0}^2}{q^2} q_\mu \right) F_1^{Bf_0}(q^2) + \frac{M_B^2 - M_{f_0}^2}{q^2} q_\mu F_0^{Bf_0}(q^2) \right], \quad (19)$$

where $P_\mu = (p + p')_\mu$ and $q_\mu = (p - p')_\mu$, and the f_0 decay constant as

$$\langle f_0 | q\bar{q} | 0 \rangle = M_{f_0} \tilde{f}_{f_0}^q \quad (20)$$

for $q \in (n, s)$. Defining $|f_0^q\rangle \equiv |q\bar{q}\rangle$, we have

$$\langle f_0^s | s\bar{s} | 0 \rangle = M_{f_0} \tilde{f}_{f_0}^s \quad \text{and} \quad \langle f_0^n | u\bar{u} | 0 \rangle = \frac{1}{\sqrt{2}} M_{f_0} \tilde{f}_{f_0}^n, \quad (21)$$

so that $\tilde{f}_{f_0}^s = \tilde{f}_{f_0}^s \cos \theta$ and $\tilde{f}_{f_0}^n = \tilde{f}_{f_0}^n \sin \theta$. Similarly we define $F_0^{Bf_0} = \sin \theta F_0^{Bf_0^d} / \sqrt{2}$, where $F_0^{Bf_0^d}$ describes the form factor to the $|d\bar{d}\rangle$ piece of the $f_0(980)$ final state.

In order to calculate the $B \rightarrow f_0$ form factor we assume the f_0 to be a $q\bar{q}$ state and use the constituent quark model (CQM) of Refs. [40, 41, 42, 43], which combines heavy quark effective theory with chiral symmetry in the light quark sector. In Refs. [40, 41], Gatto *et al.* study the $D \rightarrow \sigma\pi \rightarrow 3\pi$ and $D_s \rightarrow f_0\pi$ amplitude using the CQM model for the $D \rightarrow \sigma$ and $D_s \rightarrow f_0$ form factors and find good agreement with E791 data. This model describes interactions in terms of

effective vertices between a light quark, a heavy quark, and a heavy meson. The model depends on both its UV and IR cutoffs. The UV cutoff Λ is set by the spontaneous chiral symmetry breaking scale Λ_χ , which is of $\mathcal{O}(1 \text{ GeV})$. This model does not include confinement, so that one has to introduce an IR cutoff $\bar{\mu}$. The constituent quark mass m , is determined by solving the Nambu Jona-Lasinio (NJL) gap equation, which, in turn, depends on the UV and IR cutoffs. We choose $\Lambda = 1.25 \text{ GeV}$ as described in Ref. [43]. Thus for fixed Λ , as the IR cutoff varies, m varies accordingly, as explicitly illustrated in Ref. [44]. For the default value of the $B \rightarrow f_0$ form factor we use $m = 0.3 \text{ GeV}$, $\bar{\mu} = 0.3 \text{ GeV}$, and $\Delta_H = 0.4 \text{ GeV}$. The parameter $\Delta_H \equiv M_H - M_Q$, where M_H is the mass of the heavy meson and M_Q is the mass of the constituent heavy quark. Explicit expressions for the polar and direct contributions to the form factor are given in Refs. [40, 41]. To assess the range of the $B \rightarrow f_0$ form factor we vary $\bar{\mu}$ in the range $[0.25, 0.35]$, as per the associated variation in m given in Ref. [44], and vary Δ_H in the range $[0.3, 0.5]$ as given in Refs. [40, 41, 42, 43]. We find that the variation in $F^{Bf_0^d}$ is mainly driven by the variation in $\bar{\mu}$. However, the error range reported in Refs. [40, 41] was apparently determined by varying Δ_H alone [45]. The default value of the $B \rightarrow f_0$ form factor, as well as its uncertainty, are given in Sec. III A.

The uncertainty in the calculation of the decay amplitude comes from both the statistical and systematic errors present in the QCD factorization approach. The uncertainties associated with different input parameters such as the scalar meson decay constants, the form factors, the quark masses, and the Gegenbauer moments of light-cone distribution amplitudes are of first kind, whereas the uncertainties associated with the $1/m_b$ -suppressed corrections are of the second kind. The theoretical uncertainties in the latter case come from the hard spectator and the weak annihilation contributions which contain endpoint divergences. The endpoint divergences X_H in the hard spectator and X_A in the annihilation terms are parameterized as [29]

$$X_{H,A} = \ln \left(\frac{M_B}{\Lambda_h} \right) (1 + \rho_{H,A} e^{i\phi_{H,A}}), \quad (22)$$

where we assume $\rho_{H,A} \leq 1$ and $\Lambda_h = 0.5 \text{ GeV}$. We note $\phi_{H,A}$ are unknown, strong-interaction phases.

We wish to determine the impact of the various theoretical uncertainties in the $B \rightarrow f_0 K$ decay amplitude on the value of $\Delta S_{f_0 K_S}$ in a quantitative way. To realize this, we begin by defining a “default model.” This consists of using the central values of the inputs given in Ref. [17, 29], as well as setting $\rho_A = \rho_H = 0$ in the parameterization of the endpoint divergences. With this in place we thus determine the default values of the $A_{u,c}^{n,s}$ amplitudes. To gauge the size of the uncertainties, we perform a random scan of the allowed theoretical parameter space. That is, we include the uncertainties coming from all the input parameters. For the parameter scan, we choose the range of the input parameters by taking either 1σ , 2σ , or 3σ deviations from the central values. Once we have the maximal and minimal values of the inputs in the chosen ranges, we draw random values of the input parameters within that range. Similarly, to include the uncertainties coming from X_A and X_H we vary $\rho_{H,A}$ from 0 to 1 and $\phi_{H,A}$ from 0 to 2π . That is, we draw random values of $\rho_{H,A}$ in the range 0 to 1 and $\phi_{H,A}$ in the range 0 to 2π .

III. RESULTS AND DISCUSSION

A. Inputs

For definiteness, we summarize the parameter choices of our default model. We employ a renormalization scale of $\mathcal{O}(m_b/2)$; namely, we choose $\mu = 2.1$ GeV, so that the value of the strong coupling constant in NLO at this scale is $\alpha_s(2.1 \text{ GeV}) = 0.286$. To realize this, we work with $N_f = 5$ throughout, after Ref. [29], and choose $\Lambda^{(5)} = 0.225$ GeV, which corresponds to $\alpha_s(M_Z) = 0.118$. As a check of the accuracy of NLO precision in this context, we compare our results with those computed at $\mu = 4.2$ GeV, for which we note $\alpha_s(m_b) = 0.224$. For the electromagnetic coupling constant, we use $\alpha^{-1} = 129$ and neglect the Q^2 evolution of α as in Ref. [29]. To realize the Wilson coefficients, we follow the procedures of Ref. [29], using $m_t(m_t) = 167$ GeV, $M_W = 80.4$ GeV, and $\sin^2 \theta_W = 0.23$ [29]¹ and verify the leading-order (LO) and NLO Wilson coefficients they report through explicit computation. We also use the values $\rho_A = \rho_H = 0$ to fix the default values of the hard spectator and annihilation terms. We fix the value of the b quark mass at the scale $\mu = 2.1$ GeV to be $m_b(2.1 \text{ GeV}) = 4.88 \pm 0.08$ GeV, which corresponds to $m_b(m_b) = 4.2 \pm 0.07$ GeV [46] using the two-loop expression for the running quark mass [34]. The error in $m_b(2.1 \text{ GeV})$ is calculated using the maximum and the minimum value of m_b at the $\mu = m_b$ scale. Similarly the value of $m_s(m_b) = 0.077 \pm 0.017$ GeV corresponds to $m_s(2.1 \text{ GeV}) = 0.090 \pm 0.020$ GeV, after Ref. [30]. For the meson masses we use $M_B = 5.2795(5)$ GeV, $M_{K^0} = 0.497648(22)$ GeV, and $M_{f_0} = 0.980(10)$ GeV, as given in Ref. [46], where the uncertainty in the last digits is indicated by the number in parentheses. Similarly, the mean life of B meson is $\tau_B = 1.530(9) \times 10^{-12}$ s [46], and $G_F = 1.16637(1) \times 10^{-5}$ GeV⁻² [46]. The errors in these empirical quantities are unimportant for our purposes, so that we neglect them in our random scan. The CKM matrix elements, taken from [47] are,

$$\begin{aligned}
 |V_{ub}| &= 0.00357_{-0.00017}^{+0.00017}, & |V_{us}| &= 0.22653_{-0.00077}^{+0.00075} \\
 |V_{cb}| &= 0.0405_{-0.0029}^{+0.0032}, & |V_{cs}| &= 0.97316_{-0.00018}^{+0.00018} \\
 |\lambda_u/\lambda_c| &= 0.0205 \pm 0.0019, & |\lambda_c| &= 0.0394 \pm 0.0031 \\
 \gamma &= 76.8_{-31.5}^{+30.4}, & \beta &= 21.5_{-1.0}^{+1.0},
 \end{aligned} \tag{23}$$

where γ and β are reported in degrees. We use the uncertainties associated with the CKM matrix elements to calculate the uncertainties in $|\lambda_c|$ and $|\lambda_u/\lambda_c|$, assuming the errors are uncorrelated for simplicity. We note the angle γ is the phase associated with λ_u/λ_c , namely $\lambda_u/\lambda_c \equiv |\lambda_u/\lambda_c| e^{-i\gamma}$, and that β is the unitarity-triangle angle we defined in Sec. I. In our scan over parameter space we vary our inputs within 2σ and 3σ of their default values as well. In the case of the CKM parameters we use the ranges as reported in Ref. [47] for $|V_{ik}|$, γ , and β for $\pm 2\sigma$ and $\pm 3\sigma$ as appropriate; it is worth noting, in particular, that γ when ranged over a 3σ variation is never negative.

¹ Repeating our calculation with $m_t = 172.7$ GeV, as per Ref. [46], and following the procedures described in text yield $\Delta S_{f_0 K_S} = 0.0269$, $C_{f_0 K_S} = -0.00557$, and $\text{Br}(f_0 K_S) = 13.6 \times 10^{-6}$ in place of the values reported in Eq. (31). We can safely neglect this update in our parameter scans.

The other inputs are taken from Refs. [17, 29, 48] and are given as follows. All the scale-dependent quantities in the scalar sector are evaluated at $\mu = 2.1 \text{ GeV}$ as per Ref. [17]. The ratio of charm quark mass to the b quark mass is taken from Ref. [48]; the resulting value of the charm quark mass encompasses the value recommended in Ref. [46]. The value of the mixing angle is taken from Ref. [17]. All the other input parameters are taken from Ref. [29].

$$\begin{aligned}
B_1 &= -0.54 \pm 0.06, & B_3 &= 0.01 \pm 0.04, \\
\alpha_1^K &= 0.3 \pm 0.3, & \alpha_2^K &= 0.1 \pm 0.3, \\
\lambda_B &= 0.35 \pm 0.15 \text{ GeV}, & f_B &= 0.20 \pm 0.03 \text{ GeV}, \\
F_0^{BK} &= 0.35 \pm 0.03, & f_K &= 0.16 \text{ GeV}, \\
\bar{f}_{f_0} &= 0.460 \pm 0.025 \text{ GeV}, & \theta &= 152.5 \pm 12.5^\circ, \\
m_c/m_b &= 0.27 \pm 0.06, & m_q/m_s &= 0.0413.
\end{aligned} \tag{24}$$

We note that $m_q = (m_u + m_d)/2$ and that we neglect the error in m_q/m_s . This amounts to neglecting the error in the light-quark mass m_q , since we include the error in the strange quark mass. This we may safely do as we employ m_q/m_s in the evaluation of r_χ^K exclusively; we note that mass differences of $\mathcal{O}(m_d - m_u)$ are tantamount to the inclusion of isospin-breaking effects, which are numerically unimportant to us here. Explicit expressions for the leading-twist, light-cone distribution amplitudes of the light mesons are given in Eq. (A1), where we note B_1 and B_3 are the first and third Gegenbauer moments of the $f_0(980)$ and α_1^K and α_2^K are the first and second Gegenbauer moments of the kaon. Although all the Gegenbauer moments are scale-dependent in principle, the inclusion of such variations is beyond the accuracy of the NLO treatment we effect here, so that we neglect such refinements. The first inverse moment of the B meson light-cone distribution amplitude, λ_B , is defined by $\int_0^1 dx \Phi_B(x)/x = M_B/\lambda_B$, where $\Phi_B(x)$ is one of two twist-2 light-cone distribution amplitudes of the B meson [29, 30]. We term f_B , F_0^{BK} , f_K , and f_{f_0} the B meson decay constant, the $B \rightarrow K$ form factor, the K meson decay constant, and the scalar decay constant, respectively. The given value of f_{f_0} is specific to the assumed $q\bar{q}$ structure of f_0 ; we recall θ is the mixing angle of Eq. (18). For our inputs, we note that the ratios r_χ^M for the K meson and f_0 meson, are

$$r_\chi^K = 1.08, \quad \bar{r}_\chi^{f_0} = 0.402. \tag{25}$$

Our default value of the $B \rightarrow f_0$ form factor is

$$F_0^{Bf_0^d} = 0.284, \tag{26}$$

where we use the CQM model and the parameters $m = 0.3 \text{ GeV}$, $\bar{\mu} = 0.3 \text{ GeV}$, and $\Delta_H = 0.4 \text{ GeV}$. Cheng et al. [17] assert that the $F_0^{Bf_0^d}$ form factor should be comparable in size to the $B \rightarrow \pi$ form factor, and we find this to be consistent with our own numerical estimate. We calculate the error in the $B \rightarrow f_0$ form factor by varying $\bar{\mu}$ in the range $[0.25, 0.35]$ and Δ_H in the range $[0.3, 0.5]$. We find that the variation in $F_0^{Bf_0^d}$ with respect to Δ_H is small compared to the variation with respect to $\bar{\mu}$. That is, varying Δ_H over our chosen range makes $F_0^{Bf_0^d}$ range over the values $[0.28, 0.29]$. Varying $\bar{\mu}$ over its chosen range as well, we find that $F_0^{Bf_0^d}$ ranges from $[0.23, 0.46]$. For the random

scan we use the range $[0.23, 0.46]$ for our 1σ scan and triple its range, to yield $[0.0048, 0.69]$ for our 3σ scan.

The coefficients $a_i^p(f_0 K)$, $a_{6,8}^p(K f_0)$ and b_i are calculated at the scale $\mu = 2.1$ GeV using Eqs. (16) and (17), as well as the formulae in Ref. [29], to yield

$$\begin{aligned}
a_4^u &= -0.0261 - i0.0208, & a_4^c &= -0.0340 - i0.0110, \\
a_6^u &= -0.0581 - i0.0185, & a_6^c &= -0.0641 - i0.00842, \\
a_8^u &= (76.6 - i0.434) \times 10^{-5}, & a_8^c &= (76.5 - i0.259) \times 10^{-5}, \\
a_{10}^u &= (-172 + i130) \times 10^{-5}, & a_{10}^c &= (-172 + i130) \times 10^{-5}, \\
a_{6,8}^p(K f_0) &= a_{6,8}^p(f_0 K), \\
b_3(f_0 K_S) &= -0.0506, & b_3(K_S f_0) &= 0.0264, \\
b_{3,EW}(f_0 K_S) &= -0.00133, & b_{3,EW}(K_S f_0) &= -0.000768,
\end{aligned} \tag{27}$$

Our formulae for b_3 and b_{3EW} differ slightly from those given in Ref. [17, 29], as we detail in App. A, though the numerical differences are negligible. Now that we have all the input parameters, we can calculate the default value of the $A_{u,c}^{n,s}$ amplitudes using Eq. (12). We find

$$\begin{aligned}
A_u^n &= (-8.12 + i0.438) \times 10^{-8} \text{ GeV}, & A_c^n &= (-7.67 - i0.821) \times 10^{-8} \text{ GeV}, \\
A_u^s &= (-84.7 - i24.2) \times 10^{-8} \text{ GeV}, & A_c^s &= (-92.5 - i11.0) \times 10^{-8} \text{ GeV},
\end{aligned} \tag{28}$$

If we ignore the annihilation terms from the $B \rightarrow f_0 K_S$ decay amplitude, we find

$$\begin{aligned}
A_u^n &= (-12.5 + i0.438) \times 10^{-8} \text{ GeV}, & A_c^n &= (-12.1 - i0.821) \times 10^{-8} \text{ GeV}, \\
A_u^s &= (-76.4 - i24.2) \times 10^{-8} \text{ GeV}, & A_c^s &= (-84.3 - i11.0) \times 10^{-8} \text{ GeV},
\end{aligned} \tag{29}$$

If we ignore all the $1/m_b$ power suppressed terms in the $B \rightarrow f_0 K_S$ decay amplitude, we find

$$\begin{aligned}
A_u^n &= (-12.1 + i0.438) \times 10^{-8} \text{ GeV}, & A_c^n &= (-11.7 - i0.821) \times 10^{-8} \text{ GeV}, \\
A_u^s &= (-76.4 - i24.2) \times 10^{-8} \text{ GeV}, & A_c^s &= (-84.3 - i11.0) \times 10^{-8} \text{ GeV},
\end{aligned} \tag{30}$$

For our default parameter set, the amplitudes mediated by the $s\bar{s}$ component of the $f_0(980)$ are numerically dominant, and the various contributions coming from the power-suppressed terms are small corrections to the leading power contributions. However, these power corrections suffer endpoint divergences, and their estimate is uncertain; they could well affect the value of $\Delta S_{f_0 K_S}$. We shall consider this possibility in detail in Sec. III B. We note that the dominance of the penguin contributions associated with the strange quark component of the f_0 emerges because the a_4 and a_6 interfere destructively exclusively in the decay to the nonstrange component of the f_0 , as we can see from Eq. (12). Moreover, we note that the contribution coming from the annihilation amplitude in this case is smaller than the contribution coming from the penguin amplitude, so that the $B \rightarrow f_0 K_S$ decay amplitude is dominated by the $s\bar{s}$ component of the f_0 .

B. Two-body Decay Results

Using the default values of the $A_{u,c}^{n,s}$ amplitudes we can easily calculate $d_{f_0 K_S}$ and thus $\Delta S_{f_0 K_S}$ and $C_{f_0 K_S}$ using Eq. (6) and Eq. (7). We compute the values of $\Delta S_{f_0 K_S}$, $C_{f_0 K_S}$, and the branching

ratio (Br) for the two-body decay as discussed in Sec. II. For our default parameter set we find

$$\Delta S_{f_0 K_S} = 0.0269, \quad C_{f_0 K_S} = -0.00561, \quad \text{Br}(f_0 K_S) = 13.4 \times 10^{-6}. \quad (31)$$

We did the same calculation ignoring the annihilation terms, for which we find

$$\Delta S_{f_0 K_S} = 0.0268, \quad C_{f_0 K_S} = -0.00584, \quad \text{Br}(f_0 K_S) = 12.4 \times 10^{-6}. \quad (32)$$

Alternatively, if we neglect all $1/m_b$ suppressed terms we find

$$\Delta S_{f_0 K_S} = 0.0268, \quad C_{f_0 K_S} = -0.00587, \quad \text{Br}(f_0 K_S) = 12.3 \times 10^{-6}. \quad (33)$$

We have done the same calculation at the $\mu = m_b$ scale, and our results are very similar to those given in Eq. (31), Eq. (32), and Eq. (33). That is, we find the values of $\Delta S_{f_0 K_S}$ are 0.0269, 0.0269, and 0.0269, respectively, whereas the values of $C_{f_0 K_S}$ are -0.00603 , -0.00621 , and -0.00623 , respectively. However the value of the branching ratio does change, giving 10.3×10^{-6} , 9.69×10^{-6} , and 9.63×10^{-6} , respectively. It is evident from our numerical estimates that $\Delta S_{f_0 K_S}$ and $C_{f_0 K_S}$ and the two body branching ratio receive little contribution from the annihilation terms or, indeed, from any of the $1/m_b$ suppressed terms. That is what we expect since the $B \rightarrow f_0 K_S$ decay amplitude is driven by the s -quark component of the f_0 ; the leading power contributions to the $A_{u,c}^s$ amplitudes are much larger than the contributions coming from the power suppressed terms, and $\Delta S_{f_0 K_S}$ and $C_{f_0 K_S}$ depend only on the ratio of the $A_{u,c}^{n,s}$ amplitudes $d_{f_0 K_S}$. However, the branching ratio is controlled by the square of the sum of the amplitudes. Thus any change in the size of the amplitudes themselves will definitely change the branching ratio; this explains why our branching ratios are more sensitive to the value of μ . Our default value of the branching ratio is not consistent with the experimental value of $(5.8 \pm 0.8) \times 10^{-6}$ [7] obtained by BaBar and Belle [49, 50], so that the default set of input parameters we employ can not explain the experimental data. This does not falsify our approach per se, as it is reasonable to think that we can compute the ratio of amplitudes $d_{f_0 K_S}$ more accurately than the $A_{u,c}^{n,s}$ amplitudes alone. We also find that we are able to confront the empirical branching ratio successfully in our scan of the theoretical parameter space.

The numerical values of $\Delta S_{f_0 K_S}$ and $C_{f_0 K_S}$ for $B \rightarrow f_0 K_S$ decay are calculated by Ref. [17] as well, for which they find

$$\Delta S_{f_0 K_S} = 0.023, \quad C_{f_0 K_S} = -0.008. \quad (34)$$

Our default values of $\Delta S_{f_0 K_S}$ and $C_{f_0 K_S}$ for $B \rightarrow f_0 K_S$ decay are similar to those in Ref. [17], but they are not exactly same. We note that we also differ in our computed values of $a_i^p(f_0 K)$ and $a_{6,s}^p(K f_0)$, though this emerges, at least in part, because they employ a value of $\alpha_s(\mu = 2.1 \text{ GeV})$ appropriate to $N_f = 4$.

Our default values of $\Delta S_{f_0 K_S}$ and $C_{f_0 K_S}$ are small and that is what we expect from the SM point of view. In the QCD factorization approach the uncertainties in the calculation of the decay amplitude come from the input parameters as well as from the $1/m_b$ suppressed terms. We would like to establish the range of $\Delta S_{f_0 K_S}$ and $C_{f_0 K_S}$ possible from SM physics using the effect of the various uncertainties in the $B \rightarrow f_0 K_S$ decay amplitude. Thus it is necessary to include the corrections arising from the uncertainties associated with all the input parameters, including those in the scalar

meson decay constants, the form factors, the quark masses, the CKM elements, and the Gegenbauer moments of the light-cone distribution amplitudes. Since the quark structure of the f_0 is not well known, we are particularly interested in whether the uncertainties in the $B \rightarrow f_0$ form factor and the f_0 scalar decay constant impact the value of $\Delta S_{f_0 K_S}$ in a significant way. Additional systematic uncertainties in our calculation come from the power corrections which contain endpoint divergences; our estimate of these is uncertain. As we have noted, too, the branching ratio we compute from our default parameter set does not confront the experimental branching ratio successfully, though this is not necessary to describe $\Delta S_{f_0 K_S}$ well.

To see the effect of the above mentioned uncertainties on the various observables, we perform a random scan of the allowed theoretical parameter space. The central values of the inputs and the uncertainties associated with them are in Eq. (23), Eq. (24), and Eq. (26). For the parameter scan, we choose the range of these input parameters by taking 1σ and 3σ variations from the central values. Once we have the maximal and minimal values of the inputs in the range mentioned above, we draw random values of the input parameters in the chosen range. To include the uncertainties coming from the hard spectator and the weak annihilation terms we vary $\rho_{H,A}$ from 0 to 1 and $\phi_{H,A}$ from 0 to 2π . That is, we draw random values of $\rho_{H,A}$ in the range 0 to 1 and $\phi_{H,A}$ in the range 0 to 2π . We use the public domain random number generator “rannyu” throughout; note Ref. [51] for a discussion of suitable inputs. Each chosen parameter set corresponds to a theoretical model, and we have plotted the various combination of $\Delta S_{f_0 K_S}$ and $C_{f_0 K_S}$ for 500,000 models for a particular seed, just for illustration, for parameter ranges fixed at 1σ and 3σ from their central values in Fig. 1. The box-like shapes of the resulting regions suggest that there is little correlation between $\Delta S_{f_0 K_S}$ and $C_{f_0 K_S}$. That means $|d_{f_0 K_S}|$ is small, and $\Delta S_{f_0 K_S}$ and $C_{f_0 K_S}$ are mainly driven by $\text{Re}(d_{f_0 K_S})$ and $\text{Im}(d_{f_0 K_S})$, respectively, as we can see from Eqs. (6) and (7).

We did a random scan for two different seeds and for each seed we use 100,000 and 500,000 different theoretical models. We determine the range in $\Delta S_{f_0 K_S}$ which results, or indeed of any observable, by evaluating the extremal values which emerge from the parameter scan. This makes the results sensitive, in principle, to the detailed manner in which the scan is effected. The resulting range in $\Delta S_{f_0 K_S}$ varies little for different values of the seed and for the different numbers of theoretical models if we choose the input parameters within 1σ of the central values. For example, the range of $\Delta S_{f_0 K_S}$ for a 1σ scan is found to be $[0.017, 0.034]$ and $[0.016, 0.035]$ for two different seeds from a sample of 500,000 parameter sets. However, the range of $\Delta S_{f_0 K_S}$ does change significantly with seed if we choose the input parameters to range within either 2σ or 3σ of the central values. For example, the range of $\Delta S_{f_0 K_S}$ in the scan over a 3σ variation is found to be $[-0.41, 0.29]$ and $[-0.34, 0.20]$ for two different seeds from a sample of 500,000 parameter sets. It is evident from our scan that though the range of $\Delta S_{f_0 K_S}$ is small for 1σ variations, it is large for 3σ variations. No color-suppressed tree amplitude contributes to the $B \rightarrow f_0 K_S$ decay process, but we have large excursions in $\Delta S_{f_0 K_S}$ over small regions of the parameter space nevertheless. In these special regions, the P^c amplitude becomes small and drives the large values of $\Delta S_{f_0 K_S}$. However, such small values of P^c always give theoretical branching ratios which are much too small. It thus becomes crucial to apply the experimental branching ratio constraint to determine the allowed range in $\Delta S_{f_0 K_S}$ within the SM. We recall that the average branching ratio for $B \rightarrow f_0 K_S$ decay process measured by Belle and BaBar [49, 50] is $(5.8 \pm 0.8) \times 10^{-6}$. We impose the branching ratio constraint in such a way that we ignore those theoretical models which are not compatible within 1σ of the experimental

branching ratio for 1σ parameter scans and within 3σ of the experimental branching ratio for the 3σ parameter scans, respectively. After we impose the empirical branching ratio constraint, the seed-averaged range of $\Delta S_{f_0 K_S}$ for our scan of models spanning 1σ and 3σ variations are found to be $[0.018, 0.033]$ and $[-0.019, 0.064]$, respectively, for the 500,000 point simulation. In this context “seed-averaged” means that we report the extremal values of $\Delta S_{f_0 K_S}$ which result from scans using two different seeds. It is interesting to note that the range in $\Delta S_{f_0 K_S}$ once the branching ratio constraint is applied is almost identical to what was found without the branching ratio constraint in the 1σ scan. This underscores our point that the branching ratio is largely independent of the value of $\Delta S_{f_0 K_S}$. We find that $C_{f_0 K_S}$ as well can range over a wide array of values giving $[-0.47, 0.51]$ and $[-0.55, 0.49]$ for two different seeds from a sample of 500,000 parameter sets within 3σ of the default values. However, after applying the branching ratio constraint, such large excursions disappear, giving the seed averaged range $[-0.045, 0.051]$ for 3σ and $[-0.013, -0.0024]$ for 1σ . We plot the various combinations of $\Delta S_{f_0 K_S}$ and $C_{f_0 K_S}$ with the branching ratio constraint for the seed used in Fig. 1, just for illustration, for a random sample of 500,000 models in Fig. 2. After applying the branching ratio constraint, we find that the range in $\Delta S_{f_0 K_S}$ and in $C_{f_0 K_S}$ depends on neither the number of parameters nor the particular seed used in the random scan. To test the accuracy of our NLO analysis, we also change the renormalization scale μ from $m_b/2$ to m_b , and we find very little variation in $\Delta S_{f_0 K_S}$ and $C_{f_0 K_S}$ once the empirical branching ratio constraint is imposed. That is, the range of $\Delta S_{f_0 K_S}$ and $C_{f_0 K_S}$ in this case are $[0.017, 0.032]$ and $[-0.012, -0.0032]$ for 1σ , respectively, whereas they are $[-0.015, 0.061]$ and $[-0.044, 0.033]$ for 3σ . The weak μ dependence we observe follows as the observables involve ratios of computed amplitudes in each case.

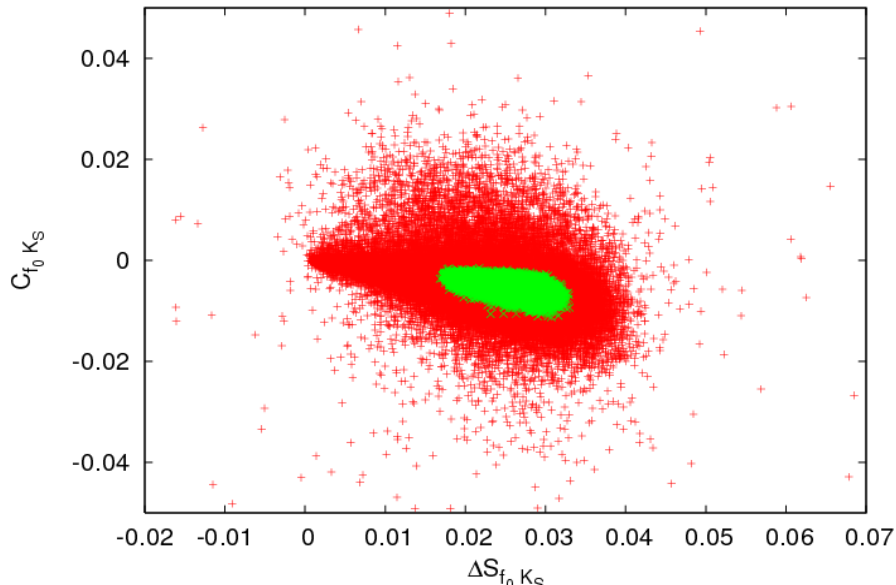


FIG. 1: Range in $\Delta S_{f_0 K_S}$ and $C_{f_0 K_S}$ from a scan of 500,000 theoretical models. The lighter interior region corresponds to a scan of the parameter space at 1σ , where the darker, larger region corresponds to a scan at 3σ . Some points in the 3σ scan fall outside the window chosen for the illustration.

To study the likelihood of various values of $\Delta S_{f_0 K_S}$ in theory space, we have plotted a histogram of $\Delta S_{f_0 K_S}$ from a sample of 100,000 and 500,000 theoretical models, after averaging over seeds, in

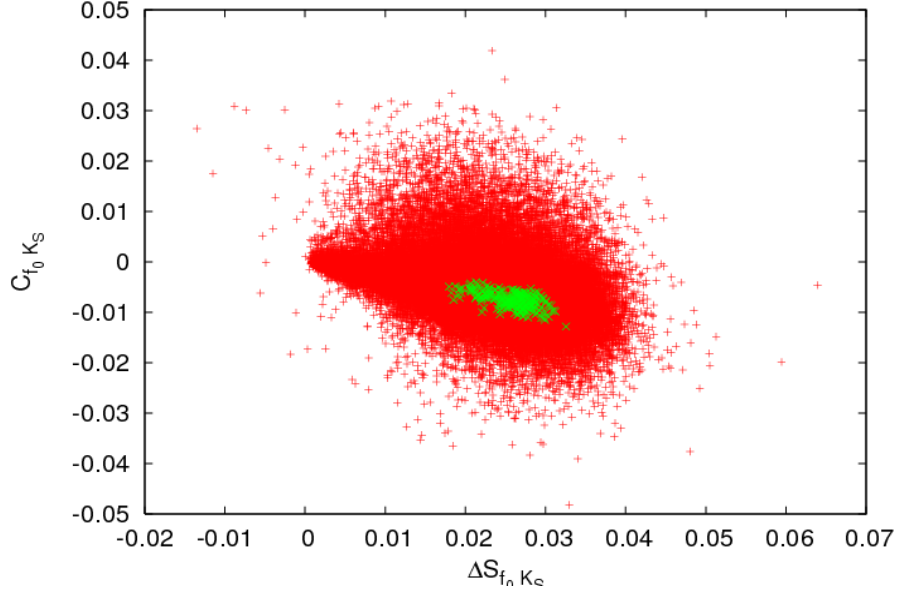


FIG. 2: Range in $\Delta S_{f_0 K_S}$ and $C_{f_0 K_S}$ from a scan of 500,000 theoretical models with the empirical branching ratio constraint imposed. The darker points represent the possible range of $\Delta S_{f_0 K_S}$ and $C_{f_0 K_S}$ within 3σ whereas the lighter points represent the range for a 1σ variation.

Fig. 3. To plot the histogram we first set a bin size and then determine the number of models which fall within each bin. Since we have different numbers of theoretical models in our random scans, to plot all of them together we divide the number of models falling in each bin by the total number of theoretical models used and choose that quantity as the ordinate of each histogram. If no points are shown, both here and in later figures, that means that no models whatsoever occupy that region of theory space. For scans employing parameters within a 1σ variation the range of $\Delta S_{f_0 K_S}$ varies little if we change the seed or the number of models used in the scan. However, it does vary notably if the parameters chosen range within 2σ or 3σ variations of their central values. In Fig. 4, we plot a histogram of $\Delta S_{f_0 K_S}$, after averaging over seeds, from a sample of 100,000 and 500,000 models taking the values of the input parameters within 3σ of their central values. It can be seen from the histogram that although the actual range of $\Delta S_{f_0 K_S}$ varies for different seeds and for different number of parameter sets, the shape of the histogram in $\Delta S_{f_0 K_S}$ does not seem to vary.

We also plot the histograms of $\Delta S_{f_0 K_S}$ after applying the branching ratio constraint, as shown in Fig. 5 and Fig. 6, and note that the shape of the histogram changes little. These results are also seed-averaged. In these figures the total number of points refer to the total number of models which satisfy the branching ratio constraint. In particular, the scale of the ordinate is not same in Fig. 5 and Fig. 6 because the total number of points which satisfy the branching ratio constraint at 1σ is small compared to those which satisfy the branching ratio constraint at 3σ . Note that the integral of these model space results over $\Delta S_{f_0 K_S}$ should yield unity in each case.

We have also studied the impact of the hadronic uncertainties alone on $\Delta S_{f_0 K_S}$ for the $B \rightarrow f_0 K_S$ decay process. To do this we set the CKM parameters to their default values and vary all the other input parameters. We include the variations in the power corrections as well. Similarly to see the impact of the CKM parameters, we set all the other hadronic inputs to their default values and vary

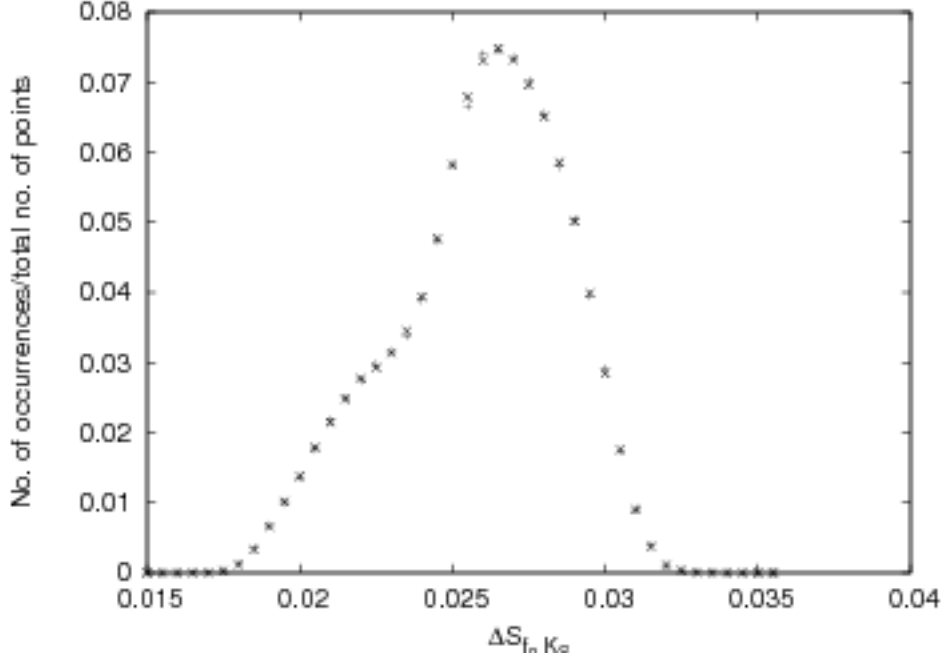


FIG. 3: Histogram for $\Delta S_{f_0 K_S}$ for a random scan employing parameters which range over 1σ of their central values. We note + denotes the scan with 100,000 models and \times denotes the scan with 500,000 models. The range of $\Delta S_{f_0 K_S}$ is the same for each case.

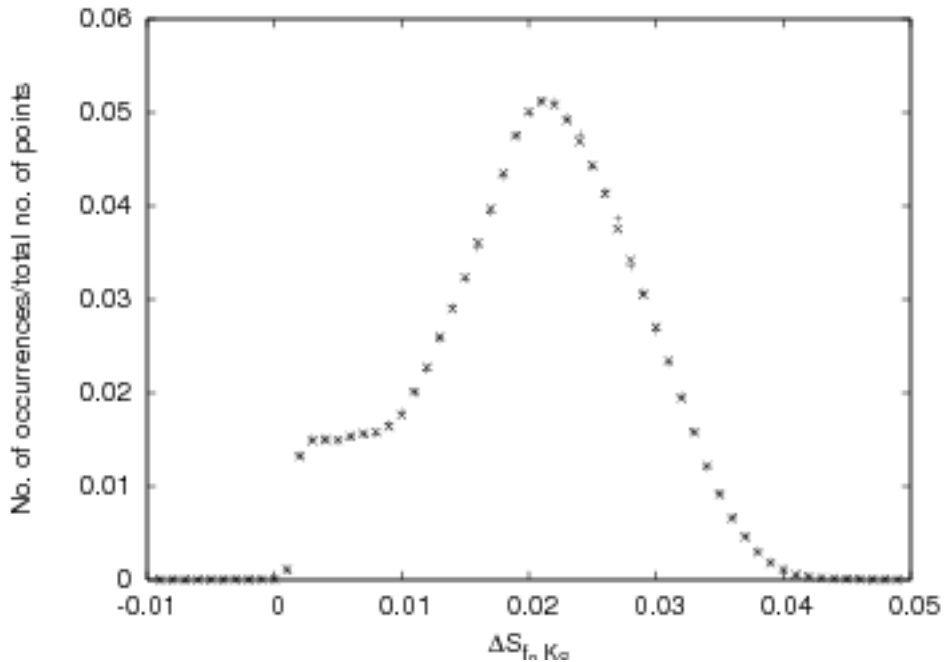


FIG. 4: Histogram for $\Delta S_{f_0 K_S}$ for a random scan employing parameters which range over 3σ of their central values. We note + denotes the scan with 100,000 models and \times denotes the scan with 500,000 models. Some points in the scan fall outside the window chosen for the illustration.

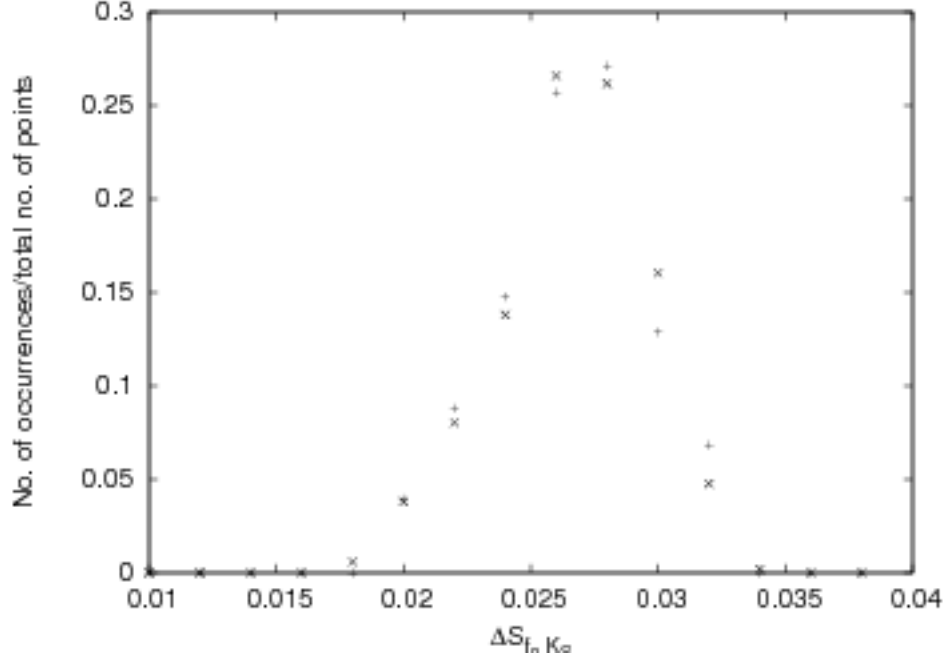


FIG. 5: Histogram for $\Delta S_{f_0 K_S}$, after that of Fig. 3, once the empirical branching ratio constraint is imposed. Here the total number of points refer to the total number of models which survive the imposed branching ratio constraint.

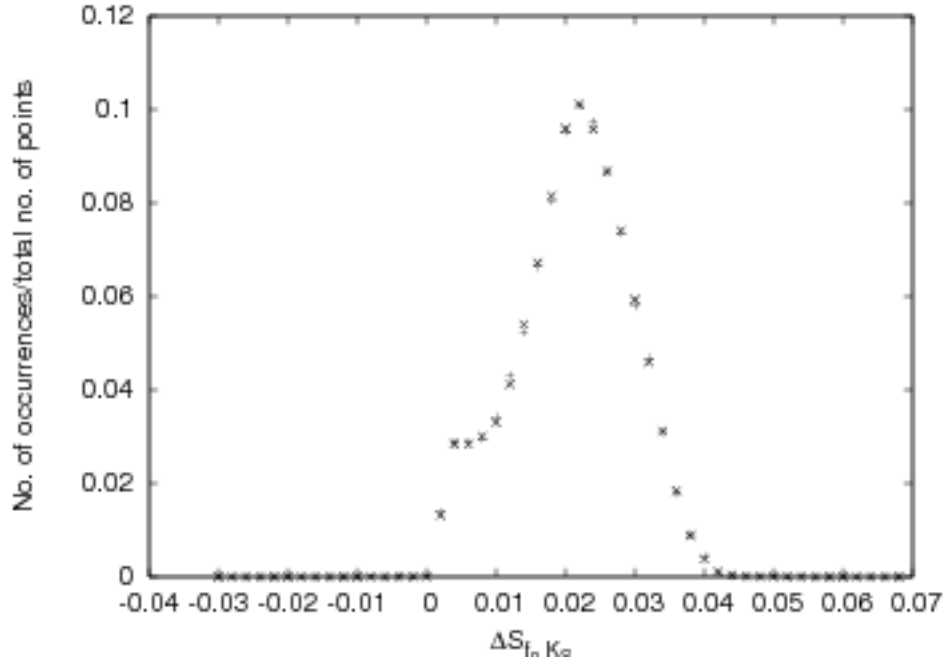


FIG. 6: Histogram for $\Delta S_{f_0 K_S}$, after that of Fig. 4, once the empirical branching ratio constraint is imposed. Here the total number of points refer to the total number of models which survive the imposed branching ratio constraint.

only the CKM parameters $|\lambda_c|$, $|\lambda_u/\lambda_c|$, γ , and β . We include the uncertainties associated with V_{ij} in an uncorrelated way to find the uncertainties in $|\lambda_c|$ and $|\lambda_u/\lambda_c|$. We perform a random scan over these CKM parameters within 1σ and 3σ of their central values as given in Eq. (23) and Ref. [47]. The associated histograms of $\Delta S_{f_0 K_S}$ for the 1σ scan are shown in Fig. 7 and Fig. 8. These results are also seed averaged. As we see from the figures, the impact of the hadronic uncertainties are very small compared to the CKM uncertainties in this case. The actual shape and range of $\Delta S_{f_0 K_S}$ is driven mainly by the CKM parameters. Since $|d_{f_0 K_S}|$ is small, the second term in the numerator of Eq. (6) is small compared to the first term — $\Delta S_{f_0 K_S}$ is mainly driven by the first term in the numerator. Both terms do tend to zero, however, as γ becomes small. Thus we expect to get very small values of $\Delta S_{f_0 K_S}$ for sufficiently small values of γ . As we can see from the histograms, variations in γ and, indeed, the CKM parameters impact the likely values of $\Delta S_{f_0 K_S}$. Since γ is never negative and the $|d_{f_0 K_S}|^2$ term is negligible, ΔS can only be negative if $\text{Re } d_{f_0 K_S} < 0$, which is an exceptionally rare occurrence.

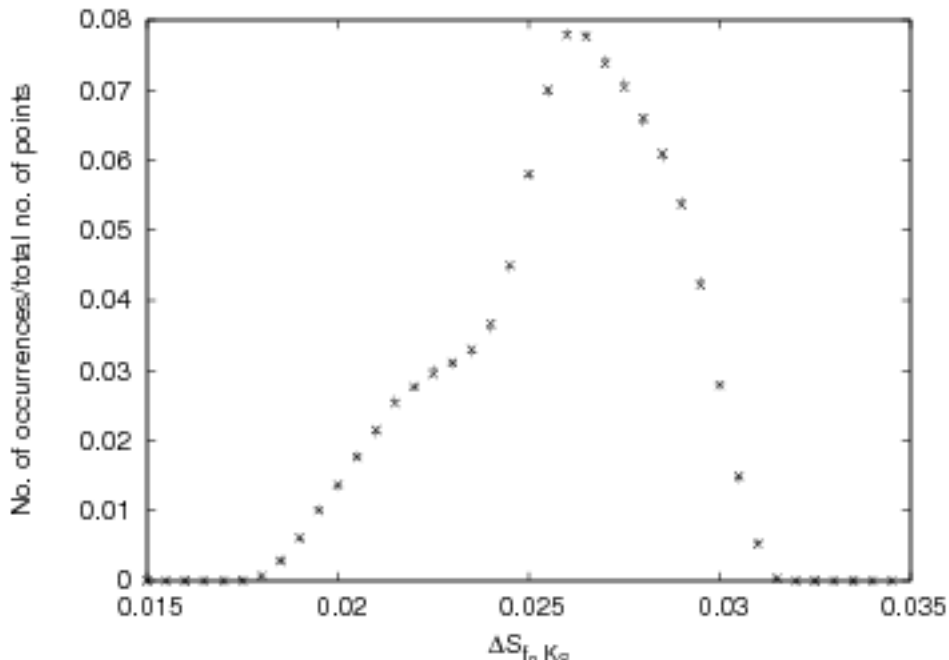


FIG. 7: Histogram for $\Delta S_{f_0 K_S}$ varying only the CKM parameters over a 1σ variation.

When we repeat this analysis for a scan in which the parameters are allowed to range over 3σ , as shown in Fig. 9 and Fig. 10, we find that the hadronic uncertainties dominate over the CKM uncertainties. This emerges, despite the detailed shapes in Fig. 9 and Fig. 10, because we use the extremal values found in the simulation to define the range. The range of $\Delta S_{f_0 K_S}$ is thus found to be $[-0.34, 0.25]$ for the hadronic uncertainties and $[0.00076, 0.039]$ for the CKM uncertainties. However, after applying the branching ratio constraint the $\Delta S_{f_0 K_S}$ range is found to be small, giving $[-0.018, 0.048]$ for the hadronic uncertainties and $[0.00080, 0.038]$ for the CKM uncertainties. In the 3σ scan the range of $\Delta S_{f_0 K_S}$ is large, so that $|d_{f_0 K_S}|$ is no longer small, for certain values of the parameter set. It is the small value of the P^c amplitude which is responsible for these large values of $|d_{f_0 K_S}|$. For $\mu = m_b$, the ranges of $\Delta S_{f_0 K_S}$ are quite similar giving $[-0.0073, 0.043]$ for

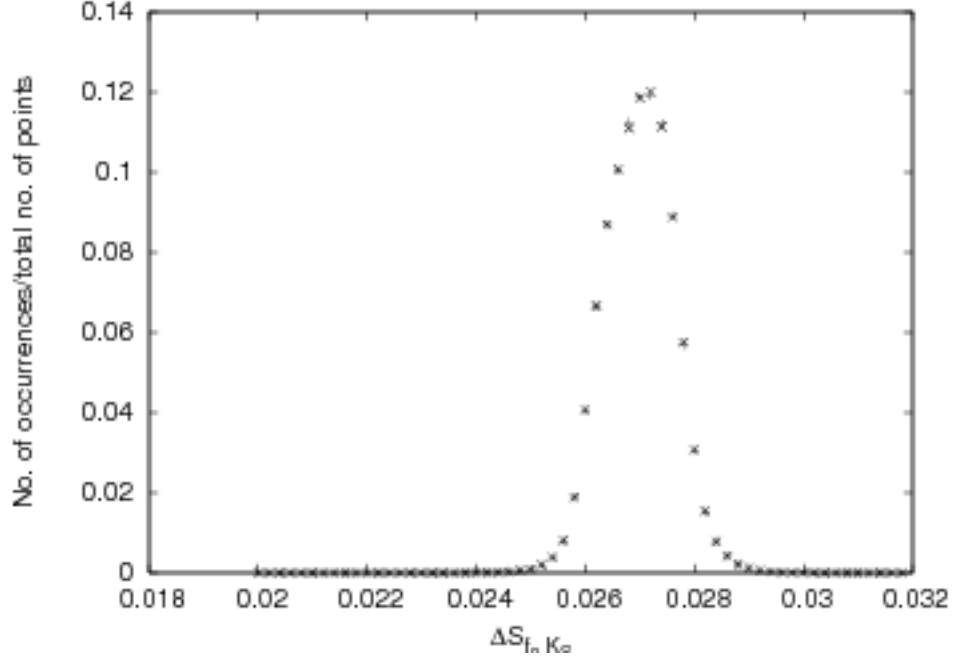


FIG. 8: Histogram for $\Delta S_{f_0 K_S}$ varying only the hadronic parameters over a 1σ variation.

the hadronic uncertainties and $[0.00075, 0.039]$ for the CKM uncertainties once the branching ratio constraint is imposed.

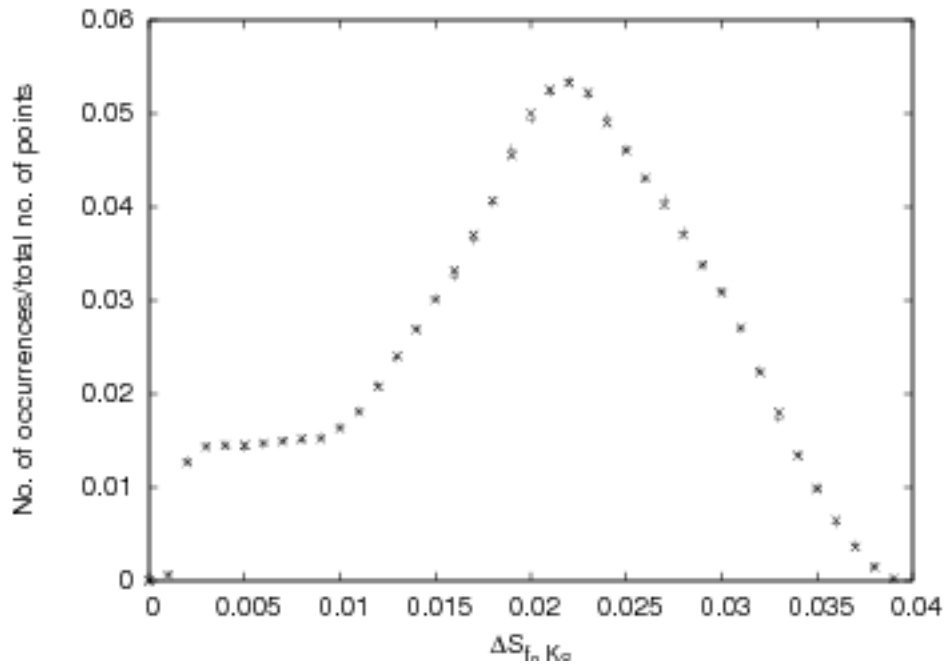


FIG. 9: Histogram for $\Delta S_{f_0 K_S}$ varying only the CKM parameters over a 3σ variation.

We have also studied the impact of the individual hadronic parameters on the value of $\Delta S_{f_0 K_S}$

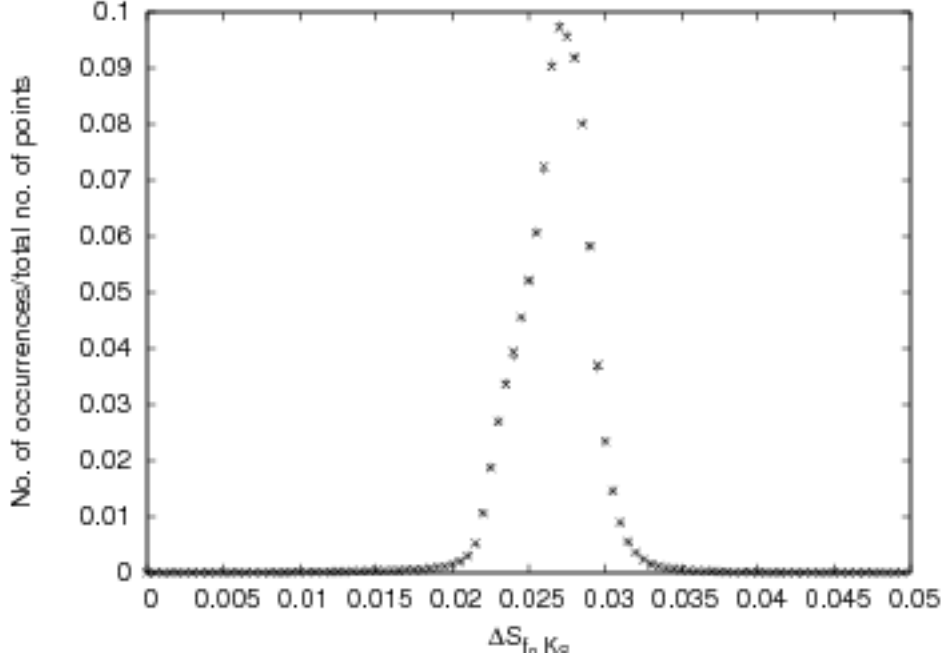


FIG. 10: Histogram for $\Delta S_{f_0 K_S}$ varying only the hadronic parameters over a 3σ variation. More points exist beyond the window chosen for the illustration.

for the $B \rightarrow f_0 K_S$ decay process. To do this we set all the other input parameters to their default values except the one which we want to study. Note that we include the variations in the power corrections as well throughout. We also use the same seed used to generate Figs. 1 and 2. We find that for any hadronic input with values in the 1σ range, the range of $\Delta S_{f_0 K_S}$ is very small. For the input parameters with values within the 3σ range, the largest excursions in $\Delta S_{f_0 K_S}$ come from the first inverse moment of the B meson distribution amplitude λ_B , which enters the $B \rightarrow f_0 K_S$ decay amplitude through the hard spectator interaction terms. However, after applying the branching ratio constraint the $\Delta S_{f_0 K_S}$ range is found to be small giving $[0.026, 0.034]$ if we employ a renormalization scale of $\mu = m_b/2$ and giving $[0.026, 0.034]$ for $\mu = m_b$. The negative values of $\Delta S_{f_0 K_S}$ found in the scan with inputs which range up to 3σ of their central values are driven by the uncertainties associated with λ_B , X_A , and X_H . To see the impact of these parameters alone on $\Delta S_{f_0 K_S}$, we set all the other input parameters to their default values and vary λ_B , X_A , and X_H within 3σ from their default values. The range of $\Delta S_{f_0 K_S}$ is quite large giving $[-0.25, 0.19]$. However, we find $\Delta S_{f_0 K_S}$ to be small and positive once we impose the branching ratio constraint, giving the range $[0.024, 0.036]$ and $[0.025, 0.036]$ for the two different renormalization scales we employ, $\mu = m_b/2$ and $\mu = m_b$, respectively. Fixing the values of λ_B , X_A , and X_H to their default values, we perform a random scan over the other input parameters within 3σ and find the range of $\Delta S_{f_0 K_S}$ to be $[-0.0015, 0.047]$. Once we impose the branching ratio constraint we find the range of $\Delta S_{f_0 K_S}$ to be $[0.00054, 0.046]$ and $[0.00037, 0.046]$ for $\mu = m_b/2$ and $\mu = m_b$, respectively. It is interesting to note that the range of $\Delta S_{f_0 K_S}$ we find by fixing the values of λ_B , X_A , and X_H to their default values, and imposed the branching ratio constraints, captures most of the range we find once we perform the scan with all the parameters within 3σ . However, we note that the extension of those scan results into negative

values come from the variations associated with λ_B , X_A , and X_H as well.

In principle, $\Delta S_{f_0 K_S}$ can have large excursions either by having a small P^c amplitude or a large P^u amplitude. The first possibility can be controlled by demanding that the theoretical model confront the empirical branching ratio successfully. As we have already noted, such small P^c amplitudes give theoretical branching ratios which are much too small, so that they can be excluded by imposing the experimental branching ratio as a constraint. We now wish to consider whether it is possible to have a large P^u amplitude without enhancing P^c as well. If it were possible, one could have a large value of $\Delta S_{f_0 K_S}$ without necessarily violating the branching ratio constraint. In the case of the default parameter set, the a_4^q , a_6^q , and a_{10}^q — a_8^q is so small as to play no role — terms interfere destructively giving small $A_{u,c}^n$ amplitudes. In this case, the hard spectator terms, which enter through the a_4^q and a_{10}^q terms, are similar in magnitude to the vertex terms in a_6^q . However, once we do a random scan over the complete theoretical parameter space, the hard spectator terms play a dominant role in enhancing the a_4^q and a_{10}^q terms, which, in turn, enhance the $A_{u,c}^n$ amplitudes. The real and imaginary parts of $a_4^q - 0.5a_{10}^q$, noting Eq. 12, e.g., can both be very large, so that the cancellation of these terms with a_6^q is no longer possible in these regions of parameter space. However, these effects act to enhance both P^u and P^c at the same time — it is not possible to have a large P^u amplitude without having a large P^c amplitude as well. Since both A_u^n and A_c^n amplitudes are large, $\Delta S_{f_0 K_S}$ is not enhanced. Thus large excursions in the hard scattering terms can not produce large excursions in the value of $\Delta S_{f_0 K_S}$.

Our primary motivation in conducting our current analysis is to determine whether it is possible to control the range of $\Delta S_{f_0 K_S}$ irrespective of the structure of the f_0 resonance. In Sec.II we noted that the structure of the f_0 impacts both the $B \rightarrow f_0$ form factor and f_0 decay constant. Thus the impact of these parameters alone on $\Delta S_{f_0 K_S}$ gives us insight as to whether we can constrain the range of $\Delta S_{f_0 K_S}$ to small values no matter the structure of the f_0 . We perform a random scan varying only these two parameters within 1σ and 3σ from their central values, both with and without the branching ratio constraint, for the particular seed used to generate Figs. 1 and 2. Without the branching ratio constraint, the range of $\Delta S_{f_0 K_S}$ is $[0.026, 0.028]$ for 1σ and $[0.025, 0.028]$ for 3σ , respectively. Once we impose the branching ratio within 3σ of the experimental value as a constraint, we find the range to be $[0.025, 0.028]$ for the scan in which the $B \rightarrow f_0$ form factor and f_0 decay constant are varied within 3σ of the central value. For $\mu = m_b$, the range of $\Delta S_{f_0 K_S}$ in this case is also very small, giving $[0.026, 0.028]$. It is evident from our analysis that the impact of the $B \rightarrow f_0$ form factor and f_0 decay constant on $\Delta S_{f_0 K_S}$ is small irrespective of the branching ratio constraint. Apparently the strange quark content of the f_0 is so important in determining $\Delta S_{f_0 K_S}$ that the particular value of the ratio of the $B \rightarrow f_0$ form factor and f_0 decay constant is quite unimportant.

IV. CONCLUSIONS

In this paper, we have analyzed the two-body decay of the B meson to one scalar meson and one pseudo-scalar meson, namely to the $f_0(980)K_S$ final state. The empirical study of this mode measures $\sin(2\beta)$ through a decay process controlled by the $b \rightarrow s$ penguin amplitude. This is

important for several reasons. First, the study of such modes is complementary to the study of the $b \rightarrow s$ transition in B_s mixing. The hint that the empirical weak phase determined from B_s mixing is larger than the SM prediction [52], if borne out, would require new sources of CP violation beyond that contained in the CKM paradigm. This makes the confirmation of, or constraints on, such effects in the $b \rightarrow s$ penguin modes crucial. Generally, we would like to assess the possible deviation of $S_f(t)$, the time-dependent CP asymmetry, from SM physics in a robust way, so that we can determine what new physics, if any, exists in these decay modes. To that end, the $f_0(980)K_S$ final state itself is of intrinsic interest. The time-dependent CP asymmetry in this case has no color-suppressed tree contribution; it is intrinsically subject to less theoretical uncertainty than modes in which such contributions are present. Moreover, its empirical study can be complementary to that of another theoretically clean process: $B \rightarrow \phi K_s$, as both modes occupy the $B \rightarrow KKK_s$ Dalitz plot. Indeed, $B \rightarrow f_0 K_s$ and $B \rightarrow \phi K_s$, assuming the ϕ to be ideally mixed, are the only known $b \rightarrow s$ penguin modes which have no color-suppressed tree contributions.

We have investigated the size of $\Delta S_{f_0 K_S}$, i.e., the deviation of $S_f(t)$ from $\sin(2\beta)$, in the $B \rightarrow f_0 K_S$ decay process in the SM using the QCD factorization approach, assuming the f_0 to be a $q\bar{q}$ state. We employ a parameter scan to probe a broad range of possible theoretical models, exploring variations in the inputs at the 3σ level and ill-known $\mathcal{O}(\Lambda_{QCD}/M_B)$ corrections with 100% uncertainty. The $B \rightarrow f_0 K_S$ decay mode has been studied by other authors within the QCD factorization approach [15, 16, 17]. Our calculation differs most significantly from this earlier work in its treatment of the $B \rightarrow f_0$ form factor, for which, for concreteness, we employ the CQM approach of Refs. [40, 41, 42, 43]. The earlier work simply asserts that the $B \rightarrow f_0$ form factor ought be comparable to that of $B \rightarrow \pi_0$. Our numerical studies support this, though we assign a large uncertainty to our assessment. The parameter scan technique we employ borrows heavily from the work of Beneke [14], in which the deviations to $S_f(t)$ from $\sin(2\beta)$ were studied for the $B \rightarrow (\pi^0 \rho^0, \eta, \eta', \phi) K_s$ decay modes. That work eschewed the $B \rightarrow f_0 K_s$ decay mode due to the uncertain $q\bar{q}$ structure of the f_0 [53]; thus we have studied the possible numerical uncertainty incurred by this with great care. Our work also differs from Beneke's in that we explore the theoretical model space for input parameters which vary within 3σ of their default values, as well as identify the parameter morphologies which give the largest excursions in $\Delta S_{f_0 K_S}$.

The assumed quark structure of the $f_0(980)$ does enter in the evaluation of the hadronic matrix elements and in the assessment of the f_0 decay constant and the $B \rightarrow f_0$ form factor in particular. We have investigated the range of $\Delta S_{f_0 K_S}$ which results from varying either the $B \rightarrow f_0$ form factor and the f_0 scalar decay constant, after imposing the branching ratio constraint, giving [0.026, 0.028] for variations within 1σ and [0.025, 0.028] for variations within 3σ . The value of $\Delta S_{f_0 K_S}$ is simply not sensitive to the value of the F^{Bf_0} form factor and the f_0 decay constant. Although we can accommodate the experimental branching ratio in a $q\bar{q}$ model of the f_0 , we can not draw conclusions concerning the structure of the f_0 on the basis of our analysis.

Let us summarize our results for the range of $\Delta S_{f_0 K_S}$ and $C_{f_0 K_S}$, which emerge from a scan of the complete theoretical parameter space, allowing for uncertainties in the infrared-cutoff dependent $\mathcal{O}(\Lambda_{QCD}/M_B)$ corrections, which we characterize by the parameters X_A and X_H . In limited regions of the parameter space, the P^c amplitude can become small, driving large excursions in $\Delta S_{f_0 K_S}$. Such excursions are removed, however, by demanding that the theoretical model confront

the empirical branching ratio up to some tolerance, that is, up to 1σ for the 1σ scans and up to 3σ for the 3σ scans. Once we demand that our theoretical models satisfy the branching ratio constraint, the possible seed averaged range in $\Delta S_{f_0 K_S}$ is greatly reduced, giving $[0.018, 0.033]$ and $[-0.019, 0.064]$ for the scans in which the parameters are allowed to range within 1σ and 3σ of their central values, respectively. In comparison, we find that $C_{f_0 K_S}$ ranges over $[-0.013, -0.0024]$ and $[-0.045, 0.051]$, respectively. Generally, we find $d_{f_0 K_S}$ to be sufficiently small that the values of $\Delta S_{f_0 K_S}$ and $C_{f_0 K_S}$ are uncorrelated, note Fig. 1. It is worth emphasizing that we estimate the ranges using the extremal values of our parameter scans. This is a conservative approach. If we were to define the range of $\Delta S_{f_0 K_S}$ to capture, e.g., 95% of the models about its most likely value in theory space, we would have much smaller ranges. Retaining our current approach, we could also sharpen our estimates once improved measurements of the branching ratio become available.

Nevertheless, let us proceed to compare our range for $\Delta S_{f_0 K_S}$ with the empirical result. The time-dependent CP asymmetry induced by the interference between $B\bar{B}$ mixing and direct decay, as well as the direct CP asymmetry, measured by Belle and BaBar [7, 54, 55] are 0.85 ± 0.07 and 0.08 ± 0.12 , respectively. The value of $\sin(2\beta)$ measured by Belle and BaBar [7] in $B \rightarrow J/\Psi K_S$ decays and related charmonium modes is 0.668 ± 0.026 , so that the empirical value of $\Delta S_{f_0 K_S}$ is 0.18 ± 0.10 for the $B \rightarrow f_0 K_S$ decay mode. Its error is substantially larger than our largest estimated value of $\Delta S_{f_0 K_S}$, so that further refinement of the experimental results is warranted. If we compare our results with those of Ref. [14] for the $B \rightarrow (\pi^0 \rho^0, \eta, \eta', \phi) K_s$ decay modes, we see that the $B \rightarrow f_0 K_S$ mode compares favorably: it yields small values of ΔS_f , as do the $B \rightarrow \phi K_s$ and $B \rightarrow \eta' K_s$ modes. Since both $B \rightarrow f_0 K_s$ and $B \rightarrow \phi K_s$ decays lack color-suppressed tree contributions, the estimation of ΔS_f should be particularly reliable, so that significant differences in the empirical values of ΔS_f in these modes could truly signal new physics.

We find that the largest single variation in our predictions of the decay amplitudes come from the uncertainty associated with the inverse moment of B meson distribution amplitude λ_B which enters the decay amplitude through the hard scattering terms. In our scans for which the parameters range over 3σ of their central values, the hard scattering terms can dominate over all other terms in the decay amplitude and produce large values of the $A_{u,c}^n$ amplitudes. The cancellation of a_4^q with a_6^q reflected in the default values of the parameter set is no longer possible for such large values of the hard scattering amplitude. This mechanism generalizes to any other mode where a_4^q and a_6^q interfere destructively. However, these large excursions in the $A_{u,c}^n$ amplitudes do not generate large excursions in $\Delta S_{f_0 K_S}$, as they also act to enhance the charm penguin amplitude. Nevertheless, the extremal values of $\Delta S_{f_0 K_S}$, and its negative values in particular, do come from the uncertainties associated with λ_B , X_A , and X_H . One expects this observation to be relevant to other $b \rightarrow s$ mode as well, though if there is a color-suppressed tree amplitude, there is more freedom for ΔS to be large.

In future studies we would like to consider how the finite width of the $f_0(980)$ resonance can impact the value of $\Delta S_{f_0 K_S}$ determined from $B \rightarrow f_0 K_S \rightarrow \pi^+ \pi^- K_S$ and $B \rightarrow f_0 K_S \rightarrow K^+ K^- K_S$ decay processes. In particular, we wish to consider the role of the $f_0 \rightarrow \pi^+ \pi^-$ and $f_0 \rightarrow K^+ K^-$ scalar form factors, as well as that of possible OZI-violating effects, in the determination of $\Delta S_{f_0 K_S}$ in a later publication [28].

Acknowledgments

We thank Timo A. Lähde, Ulf-G. Meißner, and José Oller for discussions concerning the scalar form factor in the $f_0(980)$ mass region and Martin Beneke for a discussion concerning the modelling of power corrections within QCD factorization. We also thank A. D. Polosa for useful discussions regarding the CQM model and the determination of the various form factors within this model. We thank the Institute for Nuclear Theory (INT) for gracious hospitality and acknowledge partial support from the U.S. Department of Energy under contract DE-FG02-96ER40989. S.G. thanks the SLAC theory group for gracious hospitality as well, and R.D. acknowledges a Huffaker Travel Scholarship from the University of Kentucky in generous support of his visit to the INT. S.G. also acknowledges partial support from the National Science Foundation under Grant No. NSF PHY05-51164 at its completion.

APPENDIX A: ANNIHILATION AMPLITUDES IN QCD FACTORIZATION

The weak annihilation contributions b_3 and $b_{3,EW}$ in the $B \rightarrow f_0 K_S$ decay processes are expressed as linear combinations of the annihilation amplitudes $A_{1,2,3}^{i,f}$. Explicit expressions for these amplitudes in terms of the light-cone distribution amplitudes for scalar and pseudoscalar mesons are given in [17, 29]. The general expressions for the leading-twist, light-cone distribution amplitudes for pseudoscalar and scalar mesons are written as

$$\begin{aligned}\Phi_P(x, \mu) &= 6x(1-x) \left\{ 1 + \sum_{n=1}^{\infty} \alpha_n^P(\mu) C_n^{3/2}(2x-1) \right\} \\ \Phi_S(x, \mu) &= \bar{f}_S 6x(1-x) \left\{ B_0 + \sum_{m=1}^{\infty} B_m(\mu) C_m^{3/2}(2x-1) \right\}.\end{aligned}\tag{A1}$$

Here B_0 is zero, as are all the even Gegenbauer moments, in the SU(3) limit. In order to present simple expressions for the $A_{1,2,3}^{i,f}$ amplitudes, we truncate the expansion of the pseudoscalar meson after the second Gegenbauer polynomial and that of the scalar meson after the third Gegenbauer polynomial.

We perform the integration over the light-cone distribution amplitudes in such a way that we always have $I_{xy} = I_{yx}$, where

$$\begin{aligned}I_{xy} &= \int_0^{1-\epsilon} dx \int_{\epsilon}^1 dy f(x, y), \\ I_{yx} &= \int_{\epsilon}^1 dy \int_0^{1-\epsilon} dx f(x, y).\end{aligned}\tag{A2}$$

We retain finite ϵ throughout the calculation and put $\epsilon \rightarrow 0$ only at the end to avoid dropping finite contributions. This amounts to a model of the power corrections which differs slightly from that employed previously [17, 30], giving slightly different results for $A_3^i(PS)$ and $A_3^i(SP)$. Instead of the $\pi^2/3$ found in Refs. [17, 30], we get $\pi^2/6$. That is, the annihilation amplitudes can be written

as

$$\begin{aligned}
A_1^i(PS) = & \pi\alpha_s f_K \bar{f}_{f_0}^s \left[B_1[(180 - 18\pi^2) + \alpha_1^K(3726 - 378\pi^2) + \alpha_2^K(27720 - 2808\pi^2)] \right. \\
& + B_3[(593 - 60\pi^2) + \alpha_1^K(37305 - 3780\pi^2) + \alpha_2^K(714168 - 72360\pi^2)] \\
& \left. + (3\alpha_2^K - 3\alpha_1^K + 3)[B_1(18X_A - 36) + B_3(60X_A - 190)] - 2\bar{r}_\chi^S r_\chi^K X_A^2 \right], \quad (A3)
\end{aligned}$$

$$\begin{aligned}
A_1^i(SP) = & \pi\alpha_s f_K \bar{f}_{f_0}^u \left[B_1[(-540 + 54\pi^2) + \alpha_1^K(3726 - 378\pi^2) + \alpha_2^K(-13860 + 1404\pi^2)] \right. \\
& + B_3[(-5930 + 600\pi^2) + \alpha_1^K(124350 - 12600\pi^2) + \alpha_2^K(-1190280 + 120600\pi^2)] \\
& \left. + (-3B_3 - 3B_1)[6(X_A - 1) + 18\alpha_1^K(X_A - 2) + 12\alpha_2^K(3X_A - 8)] + 2\bar{r}_\chi^S r_\chi^K X_A^2 \right], \quad (A4)
\end{aligned}$$

$$\begin{aligned}
A_3^i(PS) = & \pi\alpha_s f_K \bar{f}_{f_0}^s \left[r_\chi^K \left[18B_1(X_A^2 - 4X_A + 4 + \frac{\pi^2}{6}) + 60B_3(X_A^2 - \frac{19}{3}X_A + \frac{191}{18} + \frac{\pi^2}{6}) \right] \right. \\
& + \bar{r}_\chi^S \left[6(X_A^2 - 2X_A + \frac{\pi^2}{6}) - 18\alpha_1^K(X_A^2 - 4X_A + 4 + \frac{\pi^2}{6}) \right. \\
& \left. \left. + 36\alpha_2^K(X_A^2 - \frac{16}{3}X_A + \frac{15}{2} + \frac{\pi^2}{6}) \right] \right], \quad (A5)
\end{aligned}$$

$$\begin{aligned}
A_3^i(SP) = & \pi\alpha_s f_K \bar{f}_{f_0}^u \left[r_\chi^K \left[-18B_1(X_A^2 - 4X_A + 4 + \frac{\pi^2}{6}) - 60B_3(X_A^2 - \frac{19}{3}X_A + \frac{191}{18} + \frac{\pi^2}{6}) \right] \right. \\
& - \bar{r}_\chi^S \left[6(X_A^2 - 2X_A + \frac{\pi^2}{6}) + 18\alpha_1^K(X_A^2 - 4X_A + 4 + \frac{\pi^2}{6}) \right. \\
& \left. \left. + 36\alpha_2^K(X_A^2 - \frac{16}{3}X_A + \frac{15}{2} + \frac{\pi^2}{6}) \right] \right], \quad (A6)
\end{aligned}$$

$$\begin{aligned}
A_3^f(PS) = & \pi\alpha_s f_K \bar{f}_{f_0}^s X_A \left[r_\chi^K [6B_1(6X_A - 11) + B_3(120X_A - 374)] \right. \\
& \left. - \bar{r}_\chi^S [6(2X_A - 1) - 6\alpha_1^K(6X_A - 11) + \alpha_2^K(72X_A - 186)] \right], \quad (A7)
\end{aligned}$$

$$\begin{aligned}
A_3^f(SP) = & \pi\alpha_s f_K \bar{f}_{f_0}^u X_A \left[r_\chi^K [6B_1(6X_A - 11) + B_3(120X_A - 374)] \right. \\
& \left. - \bar{r}_\chi^S [6(2X_A - 1) + 6\alpha_1^K(6X_A - 11) + \alpha_2^K(72X_A - 186)] \right]. \quad (A8)
\end{aligned}$$

-
- [1] Y. Nir and H. R. Quinn, *Ann. Rev. Nucl. Part. Sci.* **42**, 211 (1992); I. Dunietz, *Annals Phys.* **184**, 350 (1988) and references therein.
- [2] A.B. Carter and A.I. Sanda, *Phys. Rev. Lett.* **45** (1980) 952; *Phys. Rev. D* **23** (1981) 1567.
- [3] I.I. Bigi and A.I. Sanda, *Nucl. Phys. B* **193** (1981) 85; *Nucl. Phys. B* **281** (1987) 41;
- [4] I. Dunietz and J.L. Rosner, *Phys. Rev. D* **34** (1986) 1404.
- [5] For reviews, note Ref. [1], as well as, e.g., J. Liu and L. Wolfenstein, *Phys. Lett. B* **197**, 536 (1987); Y. Nir and D.J. Silverman, *Nucl. Phys. B* **345**, 301 (1990); C. Dib, D. London, and Y. Nir, *Int. J. Mod. Phys. A* **6**, 1253 (1991); T. Goto, N. Kitazawa, Y. Okada, and M. Tanaka, *Phys. Rev. D* **53**, 6662 (1996); N.G. Deshpande, B. Dutta, and S. Oh, *Phys. Rev. Lett.* **77**, 4499 (1996); J.P. Silva and L. Wolfenstein, *Phys. Rev. D* **55**, 5331 (1997); M.P. Worah, *Phys. Rev. D* **54**, 2198 (1996); M. Gronau and D. London, *Phys. Rev. D* **55**, 2845 (1997); Y. Grossman, G. Isidori, and M. P. Worah, *Phys. Rev. D* **58**, 057504 (1998).
- [6] Y. Grossman and M. P. Worah, *Phys. Lett. B* **395**, 241 (1997); R. Fleischer, *Int. J. Mod. Phys. A* **12**, 2459 (1997); M. Ciuchini, E. Franco, G. Martinelli, A. Masiero, and L. Silvestrini, *Phys. Rev. Lett.* **79**, 978 (1997); D. London and A. Soni, *Phys. Lett. B* **407**, 61 (1997).
- [7] Heavy Flavor Averaging Group, <http://www.slac.stanford.edu/xorg/hfag>.
- [8] G. Buchalla, G. Hiller, Y. Nir, and G. Raz, *JHEP* **0509**, 074 (2005).
- [9] H. Boos, T. Mannel, and J. Reuter, *Phys. Rev. D* **70**, 036006 (2004).
- [10] H.-n. Li and S. Mishima, *JHEP* **0703**, 009 (2007).
- [11] J. Charles *et al.* [CKMfitter Group], *Eur. Phys. J. C* **41**, 1 (2005); note also <http://www.slac.stanford.edu/xorg/ckmfitter>.
- [12] M. Bona *et al.* [UTfit Collaboration], *JHEP* **0507**, 028 (2005); *JHEP* **0603**, 080 (2006); *JHEP* **0610**, 081 (2006); note also <http://www.utfig.org/>.
- [13] Y. Grossman, Z. Ligeti, Y. Nir, and H. Quinn, *Phys. Rev. D* **68**, 015004 (2003).
- [14] M. Beneke, *Phys. Lett. B* **620**, 143 (2005).
- [15] H. Y. Cheng, C. K. Chua, and A. Soni, *Phys. Rev. D* **72**, 014006 (2005).
- [16] H. Y. Cheng and K. C. Yang, *Phys. Rev. D* **71**, 054020 (2005).
- [17] H. Y. Cheng, C. K. Chua, and K. C. Yang, *Phys. Rev. D* **73**, 014017 (2006).
- [18] R. L. Jaffe, *Phys. Rev. D* **15**, 267 (1977).
- [19] J. D. Weinstein and N. Isgur, *Phys. Rev. D* **41**, 2236 (1990).
- [20] D. Lohse, J. W. Durso, K. Holinde, and J. Speth, *Phys. Lett. B* **234**, 235 (1990).
- [21] T. N. Truong, *Phys. Rev. Lett.* **61**, 2526 (1988).
- [22] A. Dobado, M. J. Herrero, and T. N. Truong, *Phys. Lett. B* **235**, 134 (1990).
- [23] J. Gasser and U.-G. Meißner, *Phys. Lett. B* **258**, 219 (1991).
- [24] J. A. Oller and E. Oset, *Nucl. Phys. A* **620**, 438 (1997) [Erratum-*ibid.* **A 652**, 407 (1999)].
- [25] U.-G. Meißner and J. A. Oller, *Nucl. Phys. A* **679**, 671 (2001).
- [26] T. A. Lähde and U.-G. Meißner, *Phys. Rev. D* **74**, 034021 (2006).
- [27] S. Gardner and U.-G. Meißner, *Phys. Rev. D* **65**, 094004 (2002).
- [28] R. Dutta, S. Gardner, T.-A. Lähde, and U.-G. Meißner, in preparation.
- [29] M. Beneke, G. Buchalla, M. Neubert, and C. T. Sachrajda, *Phys. Rev. Lett.* **83**, 1914 (1999); *Nucl. Phys. B* **606**, 245 (2001).
- [30] M. Beneke and M. Neubert, *Nucl. Phys. B* **675**, 333 (2003) and references therein.

- [31] C. W. Bauer, S. Fleming, D. Pirjol, and I. W. Stewart, Phys. Rev. D **63**, 114020 (2001).
- [32] C. W. Bauer, D. Pirjol, and I. W. Stewart, Phys. Rev. D **65**, 054022 (2002).
- [33] C. W. Bauer, D. Pirjol, and I. W. Stewart, Phys. Rev. D **67**, 071502 (2003).
- [34] G. Buchalla, A. J. Buras, and M. E. Lautenbacher, Rev. Mod. Phys. **68**, 1125 (1996).
- [35] H.-n. Li, *In the Proceedings of 5th Flavor Physics and CP Violation Conference (FPCCP 2007), Bled, Slovenia, 12-16 May 2007, pp 011* [arXiv:0707.1294 [hep-ph]].
- [36] C. W. Bauer, D. Pirjol, I. Z. Rothstein, and I. W. Stewart, Phys. Rev. D **70**, 054015 (2004).
- [37] M. Beneke, G. Buchalla, M. Neubert, and C. T. Sachrajda, Phys. Rev. D **72**, 098501 (2005).
- [38] A. Jain, I. Z. Rothstein, and I. W. Stewart, arXiv:0706.3399 [hep-ph].
- [39] P. Colangelo, G. Nardulli, N. Paver, and Riazuddin, Z. Phys. C **45**, 575 (1990); M. Ciuchini, E. Franco, G. Martinelli, and L. Silvestrini, Nucl. Phys. B **501**, 271 (1997); M. Ciuchini, R. Contino, E. Franco, G. Martinelli, and L. Silvestrini, Nucl. Phys. B **512**, 3 (1998) [Erratum-ibid.B531:656-660,1998]; M. Ciuchini, E. Franco, G. Martinelli, M. Pierini, and L. Silvestrini, Phys. Lett. B **515**, 33 (2001); C. Isola, M. Ladisa, G. Nardulli, T. N. Pham, and P. Santorelli, Phys. Rev. D **64**, 014029 (2001); S. J. Brodsky and S. Gardner, Phys. Rev. D **65**, 054016 (2002).
- [40] R. Gatto, G. Nardulli, A. D. Polosa, and N. A. Tornqvist, Phys. Lett. B **494**, 168 (2000).
- [41] A. Deandrea, R. Gatto, G. Nardulli, A. D. Polosa, and N. A. Tornqvist, Phys. Lett. B **502**, 79 (2001).
- [42] A. Deandrea, N. Di Bartolomeo, R. Gatto, G. Nardulli, and A. D. Polosa, Phys. Rev. D **58**, 034004 (1998).
- [43] A. D. Polosa, Riv. Nuovo Cim. **23N11**, 1 (2000).
- [44] D. Ebert, T. Feldmann, and H. Reinhardt, Phys. Lett. B **388**, 154 (1996).
- [45] A. D. Polosa, private communication.
- [46] W. M. Yao *et al.* [Particle Data Group], J. Phys. G **33**, 1 (2006).
- [47] Note Ref. [11]. We use the “Summer 2007” results.
- [48] A. Ali, B. D. Pecjak, and C. Greub, arXiv:0709.4422 [hep-ph].
- [49] B. Aubert *et al.* [BABAR Collaboration], Phys. Rev. D **73**, 031101 (2006).
- [50] A. Garmash *et al.* [Belle Collaboration], Phys. Rev. D **75**, 012006 (2007).
- [51] D.E. Knuth, *The Art of Computer Programming (TAOCP), Volume 2, Seminumerical Algorithms, Third Edition* (Addison-Wesley, Reading, Massachusetts, 1997), p. 102.
- [52] M. Bona *et al.* [UTfit Collaboration], arXiv:0803.0659 [hep-ph].
- [53] M. Beneke, private communication.
- [54] B. Aubert *et al.* [BABAR Collaboration], arXiv:0708.2097 [hep-ex].
- [55] K. Abe *et al.* [Belle Collaboration], Phys. Rev. D **76**, 091103 (2007).